



Finite-Time Distributive Non-Fragile Filter Design for Complex Systems with Multiple Delays, Missing Measurements and Dynamic Quantization

R. Sakthivel¹ · V. Nithya² · V. T. Suveetha¹ · F. Kong³

Received: 9 April 2021 / Revised: 17 September 2022 / Accepted: 17 September 2022

© The Author(s), under exclusive licence to Springer Science+Business Media, LLC, part of Springer Nature 2022

Abstract

This paper deals with the problem of finite-time dissipative-based distributive non-fragile filter design for a class of discrete-time complex systems subject to randomly occurring multiple delays, dynamic quantization and missing measurements. The main intention of this work is to propose a distributive non-fragile filter that ensures the stochastic finite-time boundedness together with prescribed dissipative performance in the presence of multiple delays. To characterize the random nature of delays, stochastic variables are introduced which satisfy the Bernoulli binary distribution. Moreover, the two factors such as missing measurements and dynamic quantization are implemented in the measurement signal. By employing S -procedure and constructing proper Lyapunov–Krasovskii functional, a set of linear matrix inequality (LMI)-based sufficient conditions that guarantee the stochastic finite-time boundedness with dissipative performance of the augmented filtering error system is obtained. Finally, the efficiency of the proposed distributive non-fragile filter design is proved by presenting three numerical examples including the continuous stirred tank reactor (CSTR) and a quarter-car suspension model.

✉ R. Sakthivel
krsakthivel@yahoo.com

V. Nithya
nithya.ve@gmail.com

V. T. Suveetha
suveetha94@gmail.com

F. Kong
fanchaokong88@yahoo.com

¹ Department of Applied Mathematics, Bharathiar University, Coimbatore 641046, India

² Department of Mathematics, PSG College of Arts and Science, Coimbatore 641014, India

³ School of Mathematics and Statistics, Anhui Normal University, Wuhu 241000, Anhui, China

Keywords Complex systems · Distributive non-fragile filter design · Missing measurements · Randomly occurring multiple delays · Stochastic finite-time boundedness

1 Introduction

The dynamical systems with many interacting components whose behavior is intrinsically difficult to model due to dependencies between the components which are represented in the form of complex systems. Such systems appear widely in a variety of fields such as power grid, economic systems, transportation systems and communication systems [4, 7, 11, 16–20]. On the other hand, it is well known that state variables are not available at any time for measurement, so a state estimation strategy should be used with the available measurement to estimate the unavailable states of the complex system. Moreover, the distributive filtering or state estimation problems have been received significant attention in industrial processes and control systems [1, 9, 10, 13, 21, 31, 36]. Meanwhile, in the distributive filter design, each node can accumulate required information from its neighborhood nodes. Further, it should be mentioned that distributive filtering can effectively reduce the cost and save energy significantly. In [1], the authors investigated the distributive filtering problem for a class of discrete-time T–S fuzzy systems subject to deception attacks and event-triggering protocols.

The existence of time delay is inevitable in most of the physical processes such as communication systems and biological systems. Further, the presence of delay significantly deteriorates the system performance or instantaneously leads to instability. Consequently, the studies on distributed delay and infinitely distributed delay have gained remarkable research interest in recent years [3, 5, 15, 22, 26, 32]. By employing stochastic analysis method, sufficient conditions are derived in [15] for finite-time synchronization of complex-valued neural networks error system in the presence of multiple time-varying delays and infinite distributed delays. The authors in [32] focused on H_∞ filtering problem for a class of networked systems with random distributed delays, and the random variables are assumed to follow Bernoulli distribution. However, the insertion of communication networks introduces some unavoidable technological imperfections such as dynamic quantization and missing measurements due to the unreliability of communication channels. Particularly, while comparing with a static quantizer, dynamic quantizer gives better results with their varying parametric values. For this purpose, some related studies on the dynamic quantizer in the filter design problems have been observed in [2, 12, 27, 30]. Specifically, in [30] the dynamic quantized measurement is introduced in fault detection filtering problem for uncertain linear systems. Furthermore, in [2] a fault detection filter is designed to ensure the asymptotic stability of discrete-time nonlinear impulsive switched systems with a dynamic quantizer.

It is worth mentioning that dissipative theory plays an important role in the study of system stability. Moreover, compared with H_∞ and passivity performances, dissipativity is a more general criterion. Also, it provides a less conservative and more flexible filter design since it manages a better trade-off between the gain and phase

performances. However, there are only a few results that have been proposed regarding dissipative-based filtering [24, 29, 35]. Most of the existing results in the literature regarding distributive filter design are focused on the Lyapunov asymptotic stability defined over an infinite-time interval. However, in practical applications, analyzing the behavior within a finite-time is significant and meaningful. Finite-time stability and boundedness admit that the states of the system do not exceed a certain bound during a finite-time interval. In recent years, many results on finite-time stability or boundedness are obtained [6, 8, 14, 23, 25, 28]. In [28], the authors studied finite-time H_∞ filter design problem for a class of Itô stochastic Markovian jump systems based on Lyapunov technique and LMI approach.

Based on the above discussions, a finite-time distributive non-fragile filter design problem for complex systems with multiple delays, missing measurements and dynamic quantization is investigated in this work. The main concerns of this paper are as follows:

- A dissipative-based distributive non-fragile filter design problem is investigated for a class of complex systems with stochastic multiple delays, missing measurements and dynamic quantization.
- A unified system model over the sensor nodes is proposed to describe the phenomena of missing measurements and dynamic quantization.
- By using Lyapunov stability theory, S-procedure lemma together with stochastic system analysis, a new set of sufficient conditions is established for the existence of desired distributive non-fragile filter.

Finally, the feasibility and effectiveness of the developed distributive non-fragile filter design methodology are illustrated by using numerical examples including CSTR model and a quarter-car suspension model.

2 Problem Formulation and Preliminaries

In this work, we consider the sensor network in the form of interconnection topology with ℓ number of sensor nodes. The sensor networks are distributed in the space as direct graph $\mathbb{G} = (\mathbb{V}, \mathbb{E}, \mathbb{A})$, where $\mathbb{V} = \{1, 2, \dots, \ell\}$ is the set of nodes; \mathbb{E} contained in sensors mapping set is the collection of edges and $\mathbb{A} = (a_{ij})_{n \times n}$ is the positive adjacency matrix correlated with the edges of the directed graph, i.e., $a_{ij} > 0$ implies edge $(i, j) \in \mathbb{E}$. Furthermore, the sensors are self-connected, i.e., $a_{ii} = 1$ for every $i \in \mathbb{V}$. Finally, $\mathcal{N}_i = \{j \in \mathbb{V} : (i, j) \in \mathbb{E} \text{ for all } j \in \mathbb{V}\}$ determines that sensor node i can gather data from its neighboring sensor node j .

Consider the complex system with stochastic distributed time-varying delays, infinitely distributed delays and dynamic quantization in the following form:

$$\begin{aligned}
 x(k+1) &= Ax(k) + A_{d1} \sum_{r=1}^h \beta_r(k) x(k - d_r(k)) \\
 &\quad + \xi(k) A_{d2} \sum_{\tilde{\tau}=1}^{\infty} \mu_{\tilde{\tau}} x(k - \tilde{\tau}) + B\tilde{w}(k),
 \end{aligned}$$

$$\begin{aligned} z(k) &= Lx(k), \\ x(t) &= \Phi(t), \quad -\infty \leq t \leq 0, \end{aligned} \tag{1}$$

where $x(k) \in \mathbb{R}^{n_1}$ is the state vector, $z(k) \in \mathbb{R}^{n_2}$ is the output vector, $\tilde{w}(k)$ is the disturbance input satisfying $\sum_{k=0}^{\mathcal{N}} w^T(k)w(k) \leq \varphi$, for any scalar $\varphi > 0$ and A, A_{d1}, A_{d2}, B and L are known constant matrices with proper dimensions. $d_r(k)$ ($r = 1, 2, \dots, h$) is the distributed time-varying delay which satisfies the condition $d_m \leq d_r(k) \leq d_M$, where the positive integers d_m and d_M are the lower and upper bound of the time-varying delay. The infinitely distributed time delay is represented as $\sum_{\tilde{\tau}=1}^{\infty} \mu_{\tilde{\tau}}x(k - \tilde{\tau})$, where $\mu_{\tilde{\tau}}$ ($\tilde{\tau} = 1, 2, \dots, \infty$) is greater than or equal to zero and also satisfies the convergence condition $\bar{\mu} = \sum_{\tilde{\tau}=1}^{\infty} \mu_{\tilde{\tau}} \leq \sum_{\tilde{\tau}=1}^{\infty} \tilde{\tau}\mu_{\tilde{\tau}} < +\infty$. $\Phi(t)$ is the initial condition; $\beta_r(k)$ ($r = 1, 2, \dots, h$) and $\xi(k)$ are the stochastic variables which are assumed for the distributed time-varying delay and infinitely distributed time delay, respectively. Moreover, the stochastic variables satisfy the Bernoulli distributed white sequences in the following form: $\Pr\{\beta_r(k) = 1\} = \mathbb{E}\{\beta_r(k)\} = \bar{\beta}$, $\Pr\{\beta_r(k) = 0\} = 1 - \bar{\beta}$ and $\Pr\{\xi(k) = 1\} = \mathbb{E}\{\xi(k)\} = \bar{\xi}$, $\Pr\{\xi(k) = 0\} = 1 - \bar{\xi}$. The local measurement based model of i th sensor node is considered as follows:

$$y_i(k) = C_i x(k), \quad i = 1, 2, \dots, n, \tag{2}$$

where $y_i(k) \in \mathbb{R}^{\ell_{2i}}$ is the measured output of the i th sensor, C_i is the known matrix, and it denotes the state which is to be measured.

2.1 Dynamic Quantizer

In this paper, the transmission of local measurement takes place only after quantization by considering the dynamic quantizer as the general form given in [27]. Specifically, $q_{\delta}(y_i(k))$ is the quantized signal of the local measurement $y_i(k)$ and is defined as

$$q_{\delta}(y_i(k)) = \delta(k)q\left(\frac{y_i(k)}{\delta(k)}\right) = y_i(k) + \delta(k)\left(q\left(\frac{y_i(k)}{\delta(k)}\right) - \frac{y_i(k)}{\delta(k)}\right) = y_i(k) + \vartheta_i(k), \tag{3}$$

where $\delta(k)$ is the quantized parameter of the dynamic quantizer $y_{qi}(k)$ and $q\left(\frac{y_i(k)}{\delta(k)}\right)$ is the static quantizer which satisfies the condition:

$$\|q_{\delta}(y_i(k)) - y_i(k)\| \leq \Gamma_{\delta}, \quad \text{if } \|y_i(k)\| \leq \mathcal{M}_{\delta}, \tag{4}$$

$$\|q_{\delta}(y_i(k)) - y_i(k)\| > \Gamma_{\delta}, \quad \text{if } \|y_i(k)\| > \mathcal{M}_{\delta}, \tag{5}$$

where Γ_δ represents the quantization error bound and \mathcal{M}_δ denotes the range of the static quantizer $q\left(\frac{y_i(k)}{\delta(k)}\right)$. In particular, Γ_δ and \mathcal{M}_δ are the range and quantization error bound of the dynamic quantizer $q\left(\frac{y_i(k)}{\delta(k)}\right)$, respectively.

Remark 1 The parameter $\delta(k)$ can be seen as the zooming variable according to the variation of $y_i(k)$. If $y_i(k)$ is large and the zooming variable $\delta(k)$ is decreased, then we can obtain the quantization with broadest range and quantized error bound, whereas if the zooming variable $\delta(k)$ is increased, then we can obtain the quantization with lower range and quantized error bound. Thus, the parameter $\delta(k)$ is revised only based on the system output.

Now, we introduce the complete affix of the uncertainty terms into the measurement model together with the stochastic variables as follows:

$$\bar{y}_i(k) = \lambda_{1i}(k)y_i(k) + \lambda_{2i}(k)q_\delta(y_i(k)) + D_i\tilde{w}(k), \tag{6}$$

where $\tilde{w}(k)$ is the exogenous disturbance and D_i is a matrix which is constant in the communication channel.

Let $\lambda_{1i}(k)$ and $\lambda_{2i}(k)$ be the stochastic variables that satisfy the Bernoulli distributed white sequence. Moreover, the stochastic variables $\lambda_{ci}(k)$ ($c = 1, 2$) have the property that $\sum_{c=1}^2 \lambda_{ci}(k) = 1$. Finally, the local measurement with energy constraints for the distributive filter can be defined as

$$\tilde{y}_i(k) = \Pi_{\rho_i(k)}\bar{y}_i(k), \tag{7}$$

where $\bar{y}_i(k)$ is the raw measurement and $\Pi_{\rho_i(k)}$ is the structure matrix to choose a particular component of measurement for transmission. Then, the switching signal $\rho_i(k)$ belongs to $\Phi_i = \{1, 2, \dots, n_{2i}\}$, and also, we prescribe a mapping from $\rho_i(k)$ to $\rho(k)$ for all sensors where $\rho(k) \in \Phi = \{1, 2, \dots, n_{21} \times n_{22} \times \dots \times n_{2n}\}$. In particular, when $\Pi_{\rho_i(k)} = [1 \ 0 \ 0 \ \dots \ 0]$, the first component is selected for transmission, if the second component is selected for transmission, then $\Pi_{\rho_i(k)} = [0 \ 1 \ 0 \ \dots \ 0]$, and also if both the components are selected for transmission, then $\Pi_{\rho_i(k)} = \begin{bmatrix} 1 & 0 & \dots & 0 \\ 0 & 1 & \dots & 0 \end{bmatrix}$.

2.2 Distributed Filtering

As is widely known, one of the most difficult aspects of developing distributed filters for sensor networks is combining the information available to the filter on the sensor node i from both the sensor i itself and its neighbors. Therefore, the distributive non-fragile filter is designed for the i th sensor node with filter gain uncertainties as follows:

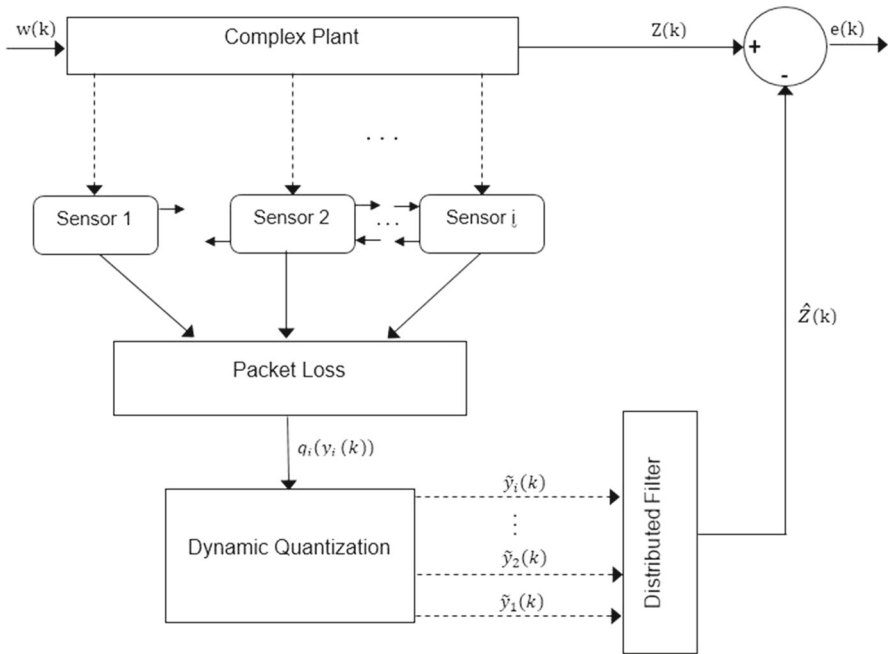


Fig. 1 Block diagram of distributed filtering error system

$$\hat{x}_i(k+1) = \sum_{j \in \mathcal{N}_i} a_{ij}(K_{ij} + \Delta K_{ij}(k))\hat{x}_j(k) + \sum_{j \in \mathcal{N}_i} a_{ij}(H_{ij} + \Delta H_{ij}(k))\tilde{y}_j(k),$$

$$\hat{z}(k) = L_{ii}x_i(k), \tag{8}$$

where $\hat{x}_j(k) \in \mathbb{R}^{n_1}$ is the filter state of the i th sensor node; $\hat{z}(k) \in \mathbb{R}^{n_2}$ is the estimated signal of $z(k)$; and K_{ij} , H_{ij} and L_{ii} are filter gain matrices to be determined. Also, the uncertain parametric matrices are defined as $[\Delta K_{ij} \ \Delta H_{ij}] = M \Delta(k) [N_{1ij} \ N_{2ij}]$, where M , N_{1ij} and N_{2ij} are constant matrices; Let $\Delta(k)$ be the time-varying matrix function which is assumed to satisfy $\Delta^T(k)\Delta(k) \leq I$. A typical block diagram of the considered distributed filtering system is shown in Fig. 1.

For our convenience, we denote

$$\bar{x}(k) = 1_{n \times n} \otimes x^T(k), \quad \hat{x}(k) = [\hat{x}_1^T(k) \ \dots \ \hat{x}_n^T(k)]^T, \quad \mathcal{A} = \text{diag}\{A, \dots, A\},$$

$$\mathcal{A}_{d1} = \text{diag}\{A_{d1}, \dots, A_{d1}\}, \quad \mathcal{A}_{d2} = \text{diag}\{A_{d2}, \dots, A_{d2}\}, \quad \mathcal{D}_i = [C_1, \dots, C_n]^T,$$

$$\mathcal{B} = [B, \dots, B]^T, \quad \mathcal{D}_i = [D_1, \dots, D_n]^T, \quad \mathcal{L} = \text{diag}\{L, \dots, L\},$$

$$\mathcal{L}_{ii} = \text{diag}\{L_{11}, \dots, L_{nn}\}, \quad \tilde{\beta}_r(k) = \beta_r(k) - \bar{\beta}_r \quad (r = 1, 2, \dots, h),$$

$$\tilde{\xi}(k) = \xi(k) - \bar{\xi},$$

$$\tilde{\lambda}_{cp}(k) = \lambda_{cp}(k) - \bar{\lambda}_{cp} \quad (c = 1, 2), \quad \Lambda_{\beta_h(k)} = \text{diag}\{\tilde{\beta}_1(k)I, \dots, \tilde{\beta}_h(k)I\},$$

$$\Lambda_{\xi(k)} = \text{diag}\{\tilde{\xi}(k)I, \dots, \tilde{\xi}(k)I\},$$

$$\begin{aligned} \Lambda_{\lambda_{cp}} &= \text{diag}\{\tilde{\lambda}_{c1}I, \dots, \tilde{\lambda}_{cn}\}, \\ \Pi_{\rho(k)} &= \text{diag}\{\Pi_{\rho_1(k)}, \dots, \Pi_{\rho_n(k)}\}, \quad \Pi_{\tilde{\lambda}_c} = \text{diag}\{\tilde{\lambda}_{c1}, \dots, \tilde{\lambda}_{cn}\}, \\ \Pi_{\tilde{\beta}_h} &= \text{diag}\{\tilde{\beta}_1I, \dots, \tilde{\beta}_hI\}, \\ \Pi_{\tilde{\xi}} &= \text{diag}\{\tilde{\xi}, \dots, \tilde{\xi}\}, \quad \theta_{\lambda_c} = \sqrt{\tilde{\lambda}_{cp}(1 + 2\tilde{\lambda}_{cp})}, \quad \theta_{\beta_h} = \sqrt{\tilde{\beta}_h(1 + 2\tilde{\beta}_h)}, \\ \theta_{\tilde{\xi}} &= \sqrt{\tilde{\xi}(1 + 2\tilde{\xi})}, \\ \hat{K}_{ij} &= \begin{cases} a_{ij}[K_{ij} + \Delta K_{ij}] & i \in \mathbb{V}, j \in \mathcal{N}_i \\ 0, & i \in \mathbb{V}, j \notin \mathcal{N}_i \end{cases} \quad \text{and} \\ \hat{H}_{ij} &= \begin{cases} a_{ij}[H_{ij} + \Delta H_{ij}] & i \in \mathbb{V}, j \in \mathcal{N}_i \\ 0, & i \in \mathbb{V}, j \notin \mathcal{N}_i \end{cases}. \end{aligned}$$

Now, let us define the error estimation as $e(k) = z(k) - \hat{z}(k)$ and the switching signal as $\rho(k) = l$. Then, from (1) to (8), the augmented filtering error system is obtained as follows:

$$\begin{aligned} \eta(k) &= \tilde{\mathcal{A}}\eta(k) + (\tilde{\beta}_h + \tilde{\beta}_h(k))\tilde{\mathcal{A}}_{d1}\eta(k - d_h(k)) + (\tilde{\xi} + \tilde{\xi}(k))\tilde{\mathcal{A}}_{d2} \sum_{\tilde{\tau}=1}^{\infty} \mu_{\tilde{\tau}}\eta(k - \tilde{\tau}) \\ &\quad + \tilde{\mathcal{D}}\tilde{w}(k) + \tilde{\mathcal{E}}v(k) + \mathcal{W}_1\eta(k) + \mathcal{W}_2\eta(k) + \mathcal{W}_E v(k), \\ e(k) &= \tilde{L}\eta(k), \\ y_i(k) &= \tilde{\mathcal{C}}_i\eta(k), \end{aligned} \tag{9}$$

where

$$\begin{aligned} \eta(k) &= [\bar{x}^T(k) \hat{x}^T(k)]^T, \\ \eta(k - d_h(k)) &= [\eta(k - d_1(k)), \eta(k - d_2(k)), \dots, \eta(k - d_h(k))]^T, \\ e(k) &= [z^T(k) - \hat{z}_1^T(k) \dots z^T(k) - \hat{z}_n^T(k)]^T, \\ \mathcal{W}_1 &= \sum_{i=1}^n \tilde{\lambda}_{1i}(k)\mathcal{W}_1^i, \quad \mathcal{W}_2 = \sum_{i=1}^n \tilde{\lambda}_{2i}(k)\mathcal{W}_1^i, \\ \mathcal{W}_E &= \sum_{i=1}^n \tilde{\lambda}_{2i}(k)\mathcal{W}_E^i, \quad \tilde{\mathcal{A}} = \begin{bmatrix} \mathcal{A} & 0 \\ \hat{H}_{ij}\Pi_l\Pi_{\tilde{\lambda}_c}\mathcal{C}_i & \hat{K}_{ij} \end{bmatrix}, \\ \tilde{\mathcal{A}}_{d1} &= \begin{bmatrix} \mathcal{A}_{d1} & 0 \\ 0 & 0 \end{bmatrix}, \quad \tilde{\mathcal{A}}_{d2} = \begin{bmatrix} \mathcal{A}_{d2} & 0 \\ 0 & 0 \end{bmatrix}, \\ \tilde{\mathcal{D}} &= \begin{bmatrix} \mathcal{B} \\ \hat{H}_{ij}\Pi_l\mathcal{D}_i \end{bmatrix}, \quad \tilde{\mathcal{E}} = \begin{bmatrix} 0 \\ \hat{H}_{ij}\Pi_l\Pi_{\tilde{\lambda}_2} \end{bmatrix}, \\ \mathcal{W}_1^i &= \begin{bmatrix} 0 & 0 \\ \hat{H}_{ij}\Pi_l\phi_l\mathcal{C}_i \end{bmatrix}, \quad \mathcal{W}_E^i = \begin{bmatrix} 0 \\ \hat{H}_{ij}\Pi_l\phi_l \end{bmatrix}, \\ \tilde{L} &= [L - L_{ii}], \quad \mathbb{E}\{\tilde{\beta}_r(k)\} = 0, \quad \mathbb{E}\{\tilde{\xi}(k)\} = 0, \quad \mathbb{E}\{\tilde{\lambda}_{ci}(k)\} = 0, \quad \mathbb{E}\{\tilde{\beta}_m^2(k)\} = \theta_{\beta_m}, \end{aligned}$$

$$\mathbb{E}\{\tilde{\xi}^2(k)\} = \theta_\beta, \quad \mathbb{E}\{\tilde{\lambda}_{ci}(k)\} = \theta_{\lambda_{ci}}.$$

Now, we present the following Lemma and Definition which are useful in obtaining the main results.

Lemma 1 (S-procedure) [30] *Given quadratic function $\eta \in \mathcal{R}^i$, $\mathbb{H}_0(\eta) = \eta^T \mathbb{J}_0 \eta$, $\mathbb{H}_1(\eta) = \eta^T \mathbb{J}_1 \eta$, $\mathbb{H}_2(\eta) = \eta^T \mathbb{J}_2 \eta$, \dots , $\mathbb{H}_g(\eta) = \eta^T \mathbb{J}_g \eta$, $\mathbb{H}_t = \mathbb{J} + t$ ($t = 1, 2, \dots, g$). Then, we have $\mathbb{H}(\eta) < 0$ with $\mathbb{J}_1(\eta) \geq 0$, $\mathbb{J}_2(\eta) \geq 0, \dots, \mathbb{J}_0(\eta) \geq 0$, if there exist scalars $\rho_1 > 0$, $\rho_2 > 0, \dots, \rho_g > 0$ satisfying*

$$\mathbb{J}_0 + \rho_1 \mathbb{J}_1 + \rho_2 \mathbb{J}_2 + \dots + \rho_g \mathbb{J}_g < 0. \quad (10)$$

Definition 1 [29] For any positive definite matrix \mathcal{J} , scalars $0 < \sigma_1 < \sigma_2, \gamma > 0$, the augmented filtering error system (9) is said to be stochastically finite-time bounded with $(\mathcal{X}, \mathcal{Y}, \mathcal{Z}) - \gamma$ dissipative performance subject to $(\sigma_1, \sigma_2, \mathbb{N}, \gamma, \mathcal{J}, \varphi)$, if it is stochastically finite-time bounded subject to $(\sigma_1, \sigma_2, \mathbb{N}, \mathcal{J}, \varphi)$, $w(k) \in l_2[0, \infty)$ and under zero initial conditions the estimation error $e(k)$ satisfies

$$\mathbb{E} \left\{ \sum_{k=0}^{\mathbb{N}} [e^T(k) \mathcal{X} e(k) + 2e^T(k) \mathcal{Y} \tilde{w}(k) + \tilde{w}^T(k) \mathcal{Z} \tilde{w}(k)] \right\} \geq \gamma \mathbb{E} \left\{ \sum_{k=0}^{\mathbb{N}} \tilde{w}^T(k) \tilde{w}(k) \right\},$$

where \mathcal{X} , \mathcal{Y} and \mathcal{Z} are real constant matrices with symmetric \mathcal{X} and \mathcal{Z} . Also, it is assumed that \mathcal{X} is less than or equal to zero, and then, we have $-\mathcal{X} = (\mathcal{X}^{-1/2})^2$.

3 Main Results

In this section, a set of sufficient conditions that guarantee the stochastic finite-time boundedness of the augmented filtering error system (9) with $(\mathcal{X}, \mathcal{Y}, \mathcal{Z}) - \gamma$ dissipative performance index will be derived. Moreover, the desired distributive non-fragile filter system is described in the form of (8) in order that the augmented filtering error system (9) in the existence of distributed time-varying delay, infinitely distributed time delay, incomplete measurements, energy constraints and dynamic quantization is stochastically finite-time bounded with $(\mathcal{X}, \mathcal{Y}, \mathcal{Z}) - \gamma$ dissipative performance index.

The following theorem discusses about stochastic finite-time boundedness with $(\mathcal{X}, \mathcal{Y}, \mathcal{Z}) - \gamma$ dissipative performance index of the augmented filtering error system (9) with known filter gain parameters.

Theorem 1 *Let $d_m, d_M, \bar{\lambda}_{1i}, \bar{\lambda}_{2i}, \bar{\beta}_r$ ($r = 1, 2, \dots, h$), $\bar{\xi}, \chi, \theta_{\lambda_{ci}}$ ($c = 1, 2$) be known positive scalars and $\mathcal{X} \leq 0$, $\mathcal{Y}, \mathcal{Z} = \mathcal{Z}^T, \mathcal{J} \geq 0$ be known constant matrices. The augmented filtering error system (9) is stochastically finite-time bounded with $(\mathcal{X}, \mathcal{Y}, \mathcal{Z}) - \gamma$ dissipative performance index subject to $(\sigma_1, \sigma_2, \mathbb{N}, \gamma, \mathcal{J}, \varphi)$ if there exist positive symmetric matrices $P_l, Q_{r,l}$ ($r = 1, 2, \dots, h$), R_l and non-negative scalars α_a ($a = 1, 2, \dots, 5$) such that the given LMIs hold for any $l = 1, 2, \dots, n_{2i} \times n_{2i} \in \Phi$:*

$$[\Upsilon]_{9 \times 9} < 0, \tag{11}$$

$$\Psi \sigma_1 + \alpha_{\mathcal{W}} \varphi < \sigma_2 \alpha_1 \chi^{-k}, \tag{12}$$

$$\alpha_1 \leq P_l \leq \alpha_2, \quad 0 < R_l < \alpha_3, \quad 0 < Q_{rl} < \alpha_{4r}, \tag{13}$$

where

$$\begin{aligned} \Upsilon_{1,1} &= -\chi P_l + (d_M - d_m + 1) \sum_{r=1}^h Q_{rl} + \bar{\mu} R_l, \\ \Upsilon_{1,4} &= -\tilde{\mathcal{L}}^T \mathcal{Y}, \quad \Upsilon_{1,6} = \tilde{\mathcal{A}}^T, \quad \Upsilon_{1,7} = \theta_{\tilde{\lambda}_{1i}} \mathcal{W}_1^{iT}, \\ \Upsilon_{1,8} &= \theta_{\tilde{\lambda}_{2i}} \mathcal{W}_2^{iT}, \quad \Upsilon_{1,9} = \tilde{\mathcal{L}}^T \sqrt{-\mathcal{X}}, \quad \Upsilon_{2,2} = -\text{diag}\{Q_{1l}, \dots, Q_{hl}\}, \\ \Upsilon_{2,6} &= \tilde{\beta}_h \tilde{\mathcal{A}}_{d1}^T + \theta_{\beta_h} \hat{\mathcal{A}}_{d1}^T, \\ \Upsilon_{3,3} &= -\frac{\chi}{\mu} R_l, \quad \Upsilon_{3,6} = \tilde{\xi} \tilde{\mathcal{A}}_{d2}^T + \theta_{\tilde{\xi}} \tilde{\mathcal{A}}_{d2}^T, \quad \Upsilon_{4,4} = -\mathcal{L} + \gamma I, \quad \Upsilon_{4,6} = \tilde{\mathcal{B}}^T, \\ \Upsilon_{5,5} &= -\frac{\mathcal{M}_\delta}{\Gamma_\delta} I, \\ \Upsilon_{5,6} &= \tilde{\mathcal{E}}^T, \quad \Upsilon_{6,6} = -P_l^{-1}, \quad \Upsilon_{7,7} = -P_l^{-1}, \quad \Upsilon_{8,8} = -P_l^{-1}, \\ \Upsilon_{9,9} &= -I, \quad \hat{\mathcal{A}}_{d1} = I_h \otimes \mathcal{A}_{d1}, \\ \Psi &= \left\{ \alpha_2 + \bar{\mu} \alpha_3 + d_M \lambda^{d_M-1} \alpha_{4r} + \lambda^{d_M} \alpha_{4r} \frac{(d_M - d_m)(d_M + d_m - 1)}{2} \right\}. \end{aligned}$$

Proof Let us consider the dynamic quantizer $q(\cdot)$ for the measured output $y_i(k)$, it is effortless to obtain that whenever $\| \frac{y_i(k)}{\delta} \| \leq \mathcal{M}_\delta$, we have

$$\left\| q\left(\frac{y_i(k)}{\delta(k)}\right) - \frac{y_i(k)}{\delta} \right\| \leq \Gamma_\delta. \tag{14}$$

Now, we consider the Euclidean norm together with inequality (9), and we obtain

$$\|v(k)\| = \left\| \delta \left(q\left(\frac{y_i(k)}{\delta(k)}\right) - \frac{y_i(k)}{\delta(k)} \right) \right\| = \delta(k) \left\| \left(q\left(\frac{y_i(k)}{\delta(k)}\right) - \frac{y_i(k)}{\delta(k)} \right) \right\| \leq \delta(k) \Gamma_\delta. \tag{15}$$

Defining $\delta(k) = \frac{\varrho}{\mathcal{M}_\delta} \|y_i(k)\|$, where ϱ is an additional scalar and satisfies $\varrho \geq 1$. Obviously, this definition guarantees that the condition $\| \frac{y_i(k)}{\delta(k)} \| \leq \mathcal{M}_\delta$ is established. Using $\delta(k)$ in Eqs. (14) and (15), we get

$$v^T(k)v(k) \leq \frac{\varrho^2 \Gamma_\delta^2}{\mathcal{M}_\delta^2} y_i^T(k) y_i(k). \tag{16}$$

Then, from (9) the aforementioned inequality can be rewritten as

$$\zeta^T(k) \Upsilon_1 \zeta(k) \geq 0, \tag{17}$$

where $\Upsilon_1 = \text{diag}\{\tilde{\mathcal{E}}^T \tilde{\mathcal{E}}, 0, 0, 0, -\frac{\mathcal{M}_\delta^2}{\varrho^2 \Gamma_\delta^2}\}$ and

$$\zeta^T(k) = \left[\eta^T(k) \eta^T(k - d_h(k)) \sum_{\tilde{\tau}=1}^{\infty} \eta^T(k - \tilde{\tau}) \tilde{w}^T(k) v^T(k) \right].$$

Now, we define the Lyapunov–Krasovskii functional for the augmented filtering error system (9) as follows:

$$V(k) = \sum_{t=1}^4 V_t(k), \tag{18}$$

where

$$\begin{aligned} V_1(k) &= \eta^T(k) P_1 \eta(k), \\ V_2(k) &= \sum_{\tilde{\tau}=1}^{\infty} \mu_{\tilde{\tau}} \eta^T(k) R_1 \eta(k), \\ V_3(k) &= \sum_{r=1}^h \sum_{j=k-d_r(k)}^{k-1} \chi^{k-j-1} \eta^T(j) Q_{r1} \eta(j), \\ V_4(k) &= \sum_{r=1}^h \sum_{j=-d_m}^{-d_h} \sum_{s=k+j}^{k-1} \chi^{k-s-1} \eta^T(s) Q_{r1} \eta(s). \end{aligned}$$

Then, by calculating the derivatives of $V(k)$ along the trajectories of augmented filtering error system (9) and taking mathematical expectation, we have

$$\begin{aligned} &\mathbb{E}\{\Delta V_1(k+1) - (\chi - 1)V_1(k)\} \\ &= \mathbb{E}\{\eta^T(k+1) P_1 \eta(k+1) - \eta^T(k) P_1 \eta(k)\}, \\ &\leq \mathbb{E}\{\eta^T(k) [\tilde{\mathcal{A}}^T P_1 \tilde{\mathcal{A}} + \mathcal{W}_1^T P_1 \mathcal{W}_1 + \mathcal{W}_2^T P_1 \mathcal{W}_2] \eta(k) \\ &\quad + \bar{\beta}_h^2 \eta^T(k - d_h(k)) \tilde{\mathcal{A}}_{d1}^T P_1 \tilde{\mathcal{A}}_{d1} \eta(k - d_h(k)) \\ &\quad + \theta_{\beta_h}^2 \eta^T(k - d_h(k)) \tilde{\mathcal{A}}_{d1}^T P_1 \tilde{\mathcal{A}}_{d1} \eta(k - d_h(k)) \\ &\quad + \bar{\xi}^2 \left(\sum_{\tilde{\tau}=1}^{\infty} \mu_{\tilde{\tau}} \eta(k - \tilde{\tau}) \right)^T \tilde{\mathcal{A}}_{d2}^T P_1 \tilde{\mathcal{A}}_{d2} \left(\sum_{\tilde{\tau}=1}^{\infty} \mu_{\tilde{\tau}} \eta(k - \tilde{\tau}) \right) \\ &\quad + \theta_{\xi}^2 \left(\sum_{\tilde{\tau}=1}^{\infty} \mu_{\tilde{\tau}} \eta^T(k - \tilde{\tau}) \tilde{\mathcal{A}}_{d2}^T \right)^T P_1 \tilde{\mathcal{A}}_{d2} \left(\sum_{\tilde{\tau}=1}^{\infty} \mu_{\tilde{\tau}} \eta(k - \tilde{\tau}) \right) \\ &\quad + \tilde{w}^T(k) \tilde{\mathcal{D}}^T P_1 \tilde{\mathcal{D}} \tilde{w}(k) + v^T(k) [\tilde{\mathcal{E}}^T P_1 \tilde{\mathcal{E}} + \mathcal{W}_E^T P_1 \mathcal{W}_E] v(k), \end{aligned} \tag{19}$$

$$\begin{aligned}
 & \mathbb{E}\{\Delta V_2(k+1) - (\chi - 1)V_2(k)\} \\
 &= \mathbb{E}\left\{\sum_{\tilde{\tau}=1}^{\infty} \mu_{\tilde{\tau}} \eta^T(k+1) R_l \eta(k+1) - \chi \sum_{\tilde{\tau}=1}^{\infty} \mu_{\tilde{\tau}} \eta^T(k) R_l \eta(k)\right\}, \\
 &\leq \mathbb{E}\left\{\bar{\mu} \eta^T(k) R_l \eta(k) - \chi \sum_{\tilde{\tau}=1}^{\infty} \mu_{\tilde{\tau}} \eta^T(k-d) R_l \eta(k-d)\right\}, \\
 &\leq \mathbb{E}\left\{\bar{\mu} \eta^T(k) R_l \eta(k) - \frac{\chi}{\bar{\mu}} \left(\sum_{\tilde{\tau}=1}^{\infty} \mu_{\tilde{\tau}} \eta(k-d)\right)^T R_l \right. \\
 &\quad \left. \times \left(\sum_{\tilde{\tau}=1}^{\infty} \mu_{\tilde{\tau}} \eta(k-d)\right)\right\} \tag{20}
 \end{aligned}$$

$$\begin{aligned}
 & \mathbb{E}\{\Delta V_3(k+1) - (\chi - 1)V_3(k)\} \\
 &= \mathbb{E}\left\{\sum_{r=1}^h \left[\sum_{j=k+1-d_r(k+1)}^k \chi^{k-j} \eta^T(j) Q_{rl} \eta(j) \right. \right. \\
 &\quad \left. \left. - \sum_{j=k-d_r(k)}^{k-1} \chi^{k-j-1} \eta^T(j) Q_{rl} \eta(j) \right]\right\}, \\
 &\leq \mathbb{E}\left\{\sum_{r=1}^h \left[\eta^T(k) Q_{rl} \eta(k) + \sum_{j=k-d_M+1}^{k-d_m} \chi^{k-j} \eta(j) Q_{rl} \eta(j) \right] \right. \\
 &\quad \left. - \chi^{d_M} \eta^T(k-d_h(k)) \text{diag}\{Q_{1l}, Q_{2l}, \dots, Q_{hl}\} \right. \\
 &\quad \left. \times \eta(k-d_h(k))\right\}, \tag{21}
 \end{aligned}$$

$$\begin{aligned}
 & \mathbb{E}\{\Delta V_4(k+1) - (\chi - 1)V_4(k)\} \\
 &= \mathbb{E}\left\{\sum_{r=1}^h \left[\sum_{j=-d_M}^{-d_m} \sum_{s=k+1+j}^k \chi^{k-s} \eta^T(s) Q_{rl} \eta(s) \right. \right. \\
 &\quad \left. \left. - \sum_{j=-d_M}^{-d_m} \sum_{s=k+j}^{k-1} \chi^{k-s-1} \eta^T(s) Q_{rl} \eta(s) \right]\right\}, \\
 &\leq \mathbb{E}\left\{\sum_{r=1}^h \left[(d_M - d_m) \eta^T(k) Q_{rl} \eta(k) \right. \right. \\
 &\quad \left. \left. - \sum_{j=k-d_M+1}^{k-d_m} \chi^{k-j} \eta(j) Q_{rl} \eta(j) \right]\right\}. \tag{22}
 \end{aligned}$$

In particular, the dissipative performance γ for the augmented filtering error system (8) has to be established. For this purpose, we consider the performance index defined in Definition 1 as

$$\mathbb{J} = \mathbb{E} \left\{ \sum_{k=0}^{\mathcal{N}} [e(k)^T \mathcal{X} e(k) + 2e^T(k) \mathcal{Y} \tilde{w}(k) + \tilde{w}^T(k) (\mathcal{Z} - \gamma I) \tilde{w}(k)] \right\}. \quad (23)$$

On the other hand, by combining (19)–(22) together with dissipative performance index (23), it is obvious to get the inequality as

$$\mathbb{E}\{\Delta V(k) - (\chi - 1)V(k) - \mathbb{J}\} \leq \mathbb{E}\{\zeta^T(k) [\Upsilon_0]_{5 \times 5} \zeta(k)\}, \quad (24)$$

where

$$\begin{aligned} [\Upsilon_0]_{1,1} &= -\chi P_l + (d_M - d_m + 1) \sum_{r=1}^h Q_{rl} + \bar{\mu} R_l + \tilde{\mathcal{A}}^T P_l \tilde{\mathcal{A}} + \theta_{\lambda_{1i}}^T \mathcal{W}_1^{iT} P_l \theta_{\lambda_{1i}} \mathcal{W}_1^i \\ &\quad + \theta_{\lambda_{2i}}^T \mathcal{W}_2^{iT} P_l \theta_{\lambda_{2i}} \mathcal{W}_2^i + \tilde{\mathcal{L}}^T \mathcal{X} \tilde{\mathcal{L}}, \\ [\Upsilon_0]_{1,4} &= -\tilde{\mathcal{L}}^T \mathcal{Y}, \quad [\Upsilon_0]_{2,2} = -\text{diag}\{Q_{1l}, \dots, Q_{hl}\} + \bar{\beta}_h^2 \tilde{\mathcal{A}}_{d1}^T Q_{rl} \hat{\mathcal{A}}_{d1} + \theta_{\beta_h}^2 \tilde{\mathcal{A}}_{d1}^T Q_{rl} \hat{\mathcal{A}}_{d1}, \\ [\Upsilon_0]_{3,3} &= -\frac{\chi}{\bar{\mu}} R_l + \bar{\xi}^2 \tilde{\mathcal{A}}_{d2}^T P_l \tilde{\mathcal{A}}_{d2} + \theta_{\xi}^T \tilde{\mathcal{A}}_{d2}^T P_l \tilde{\mathcal{A}}_{d2}, \quad [\Upsilon_0]_{4,4} = -\mathcal{Z} + \gamma I + \tilde{\mathcal{B}}^T P_l \tilde{\mathcal{B}}, \\ [\Upsilon_0]_{5,5} &= -\frac{\mathcal{M}_\delta}{\Gamma_\delta} I + \tilde{\mathcal{E}}^T P_l \tilde{\mathcal{E}}, \end{aligned}$$

In addition, by applying Lemma 1 together with $\mathbb{H}_0(\zeta) = \zeta^T(k) [\Upsilon_0]_{5 \times 5} \zeta(k)$ and $\mathbb{H}_1(\zeta) = \zeta^T(k) \Upsilon_1 \zeta(k)$, then $\mathbb{H}_0(\zeta) < 0$ holds if there exists a positive scalar ϱ such that

$$\hat{\Upsilon} = [\Upsilon_0]_{5 \times 5} + \varrho^2 \Upsilon_1 < 0. \quad (25)$$

Moreover, by implementing Schur complement lemma to inequality (25), we have

$$[\Upsilon]_{9 \times 9} < 0, \quad (26)$$

where the elements of Υ are defined in theorem statement. Thus, inequality (26) is equivalent to (11). Hence, if the inequality (11) holds, it is obvious that

$$\begin{aligned} \mathbb{E}\{\Delta V(k) - (\chi - 1)V(k) - \tilde{w}^T(k) \mathcal{W} \tilde{w}(k)\} &\leq 0, \\ \mathbb{E}\{V(k + 1) - V(k)\} &\leq (\chi - 1)\mathbb{E}\{V(k)\} + \mathbb{E}\{\tilde{w}^T(k) \mathcal{W} \tilde{w}(k)\}, \\ \mathbb{E}\{V(k + 1)\} &\leq \chi \mathbb{E}\{V(k)\} + \alpha_{\mathcal{W}} \mathbb{E}\{\tilde{w}^T(k) \tilde{w}(k)\}, \end{aligned} \quad (27)$$

where $\alpha_{\mathcal{W}} = \alpha_{\max}(\mathcal{W})$. Furthermore, there exists any positive scalar $\chi \geq 1$ such that

$\sum_{k=0}^{\mathcal{N}} w^T(k) w(k) \leq \varphi$, and then, we have

$$\mathbb{E}\{\Delta V(k)\} \leq \chi \mathbb{E}\{V(0)\} + \alpha_{\mathcal{W}} \mathbb{E}\left\{ \sum_{s=0}^{k-1} \chi^{k-s-1} w^T(s) w(s) \right\} \leq \chi \mathbb{E}\{V(0)\} + \chi^k \alpha_{\mathcal{W}} \varphi, \quad (28)$$

Moreover, from the Lyapunov–Krasovskii functional (18), we obtain

$$\begin{aligned}
 \mathbb{E}\{V(0)\} &= \mathbb{E}\left\{\sum_{\tilde{\tau}=1}^{\infty} \mu_{\tilde{\tau}} \eta^T(0) R_l \eta(0)\right\} + \mathbb{E}\left\{\sum_{r=1}^h \sum_{j=k-d_r(0)}^{-1} \chi^{-j-1} \eta^T(j) Q_{rl} \eta(j)\right\} \quad (29) \\
 &+ \mathbb{E}\left\{\sum_{r=1}^h \sum_{j=-d_M}^{-d_m} \sum_{s=j}^{-1} \chi^{-s-1} \eta^T(s) Q_{rl} \eta(s)\right\}, \\
 &\leq \alpha_2 \mathbb{E}\left\{\eta^T(0) \mathcal{J} \eta(0)\right\} + \alpha_3 \mathbb{E}\left\{\sum_{\tilde{\tau}=1}^{\infty} \mu_{\tilde{\tau}} \eta^T(0) \mathcal{J} \eta(0)\right\} \\
 &+ \alpha_{4r} \mathbb{E}\left\{\sum_{r=1}^h \sum_{j=k-d_r(0)}^{-1} \chi^{-j-1} \eta^T(j) \mathcal{J} \eta(j)\right\}, \\
 &+ \alpha_{4r} \mathbb{E}\left\{\sum_{r=1}^h \sum_{j=-d_M}^{-d_m} \sum_{s=j}^{-1} \chi^{-s-1} \eta^T(s) \mathcal{J} \eta(s)\right\}, \\
 &\leq \left\{\alpha_2 + \bar{\mu} \alpha_3 + d_M \lambda^{d_M-1} \alpha_{4r} + \lambda^{d_M} \alpha_{4r} \frac{(d_M - d_m)(d_M + d_m - 1)}{2}\right\} \sigma_1 \leq \Psi \sigma_1, \quad (30)
 \end{aligned}$$

where $\alpha_1 = \alpha_{\min}\{P_l\}$, $\chi_2 = \alpha_{\max}\{P_l\}$, $\alpha_2 = \alpha_{\max}\{R_l\}$ and $\alpha_{4r} = \alpha_{\max}\{Q_{rl}\}$ ($r = 1, 2, \dots, h$).

Moreover, from (24) we can obtain

$$\mathbb{E}\{V(k)\} \geq \mathbb{E}\{\eta^T(k) P_l \eta(k)\} \geq \mathbb{E}\{\eta^T(k) \mathcal{J}^{1/2} \tilde{P}_l \mathcal{J}^{1/2} \eta(k)\} \geq \alpha_2 \mathbb{E}\{\eta^T(k) \mathcal{J} \eta(k)\}. \quad (31)$$

Then, it is clear to obtain from (25)–(31) that

$$\mathbb{E}\{\eta^T(k) \mathcal{J} \eta(k)\} \leq \frac{(\Psi \sigma_1 + \alpha_w \varphi) \chi^k}{\alpha_1}. \quad (32)$$

Then, from (12), it is obvious that $\mathbb{E}\{\eta^T(k) \mathcal{J} \eta(k)\} < \sigma_2$ for all $k = \{1, 2, \dots, \mathbb{N}\}$. Hence, from Definition 2.1 of [6], the augmented filtering error system (9) is stochastically finite-time bounded with $(\mathcal{X}, \mathcal{Y}, \mathcal{Z}) - \gamma$ dissipative performance index subject to $(\sigma_1, \sigma_2, \mathbb{N}, \gamma, \mathcal{J}, \varphi)$. This completes the proof. \square

Next, the results are extended by taking the uncertain parameters into account to obtain the desired distributive non-fragile filter design for the augmented filtering error system (9).

Theorem 2 Let $d_m, d_M, \bar{\lambda}_{1i}, \bar{\lambda}_{2i}, \bar{\beta}_r$ ($r = 1, 2, \dots, h$), $\bar{\xi}, \chi, \theta_{\tilde{\lambda}_{ci}}$ ($c = 1, 2$) be known positive scalars and $\mathcal{X} \leq 0, \mathcal{Y}, \mathcal{Z} = \mathcal{Z}^T, \mathcal{J} \geq 0$ be known constant matrices. The augmented filtering error system (9) is stochastically finite-time bounded with $(\mathcal{X}, \mathcal{Y}, \mathcal{Z}) - \gamma$ dissipative performance index subject to $(\sigma_1, \sigma_2, \mathbb{N}, \gamma, \mathcal{J}, \varphi)$ if there exist positive definite matrices $\bar{P}_{1l}, \bar{P}_{2l}, \bar{P}_{3l}, Q_{1rl}, Q_{2rl}$ ($r = 1, 2, \dots, h$), R_{1l}

R_{2l} , any matrices Y_1, Y_2, Y_3 and positive scalars $\alpha_1, \alpha_2, \alpha_{3r}$ ($r = 1, 2, \dots, h$) such that the given LMIs together with (13) hold for every $l = 1, 2 \dots n_{2i} \times n_{2i} \in \Phi$:

$$\begin{bmatrix} [\tilde{Y}]_{9 \times 9} & \epsilon_1 \tilde{N}_{1ij}^T & \tilde{M}_1 & \epsilon_2 \tilde{N}_{2ij}^T & \tilde{M}_2 \\ * & -\epsilon_1 & 0 & 0 & 0 \\ * & * & -\epsilon_1 & 0 & 0 \\ * & * & * & -\epsilon_2 & 0 \\ * & * & * & * & -\epsilon_2 \end{bmatrix} < 0, \tag{33}$$

where

$$\begin{aligned} \tilde{Y}_{1,1} &= \begin{bmatrix} \tilde{Y}_{111} & -\chi P_{2l} \\ * & \tilde{Y}_{113} \end{bmatrix}, \quad \tilde{Y}_{1,4} = \begin{bmatrix} -\mathcal{L}^T \mathcal{Y} \\ \mathcal{L}_{Fii}^T \mathcal{Y} \end{bmatrix}, \quad \tilde{Y}_{1,6} = \begin{bmatrix} \tilde{Y}_{161} & \tilde{Y}_{162} \\ \hat{K}_{Fij}^T & \hat{K}_{Fij}^T \end{bmatrix}, \quad \tilde{Y}_{1,7} = \begin{bmatrix} \tilde{Y}_{171} & \tilde{Y}_{172} \\ 0 & 0 \end{bmatrix}, \\ \tilde{Y}_{1,8} &= \begin{bmatrix} \tilde{Y}_{181} & \tilde{Y}_{182} \\ 0 & 0 \end{bmatrix}, \quad \tilde{Y}_{1,9} = \begin{bmatrix} \mathcal{L}^T \sqrt{-\mathcal{X}} \\ -\mathcal{L}_{Fii}^T \sqrt{-\mathcal{X}} \end{bmatrix}, \quad \tilde{Y}_{2,2} = \begin{bmatrix} \tilde{Y}_{221} & 0 \\ * & \tilde{Y}_{222} \end{bmatrix}, \quad \tilde{Y}_{2,6} = \begin{bmatrix} \tilde{Y}_{261} & \tilde{Y}_{262} \\ 0 & 0 \end{bmatrix}, \\ \tilde{Y}_{3,3} &= \begin{bmatrix} -\frac{\chi}{\mu} \tilde{R}_{1l} & 0 \\ * & -\frac{\chi}{\mu} \tilde{R}_{2l} \end{bmatrix}, \quad \tilde{Y}_{3,6} = \begin{bmatrix} \tilde{Y}_{361} & \tilde{Y}_{362} \\ 0 & 0 \end{bmatrix}, \quad \tilde{Y}_{4,4} = -\mathcal{L} + \gamma I, \quad \tilde{Y}_{4,6} = \begin{bmatrix} \tilde{Y}_{461}^T \\ \tilde{Y}_{462}^T \end{bmatrix}^T, \\ \tilde{Y}_{5,6} &= \begin{bmatrix} \tilde{Y}_{561}^T \\ \tilde{Y}_{562}^T \end{bmatrix}^T, \quad \tilde{Y}_{5,8} = [\tilde{Y}_{581} \ \tilde{Y}_{482}], \quad \tilde{Y}_{6,6} = \Gamma, \quad \tilde{Y}_{7,7} = \Gamma, \quad \tilde{Y}_{8,8} = \Gamma, \quad \tilde{Y}_{9,9} = \begin{bmatrix} -I & 0 \\ * & -I \end{bmatrix}, \\ \Gamma &= \begin{bmatrix} \tilde{\Gamma}_1 & \tilde{\Gamma}_2 \\ * & \tilde{\Gamma}_3 \end{bmatrix}, \quad \tilde{Y}_{111} = -\chi P_{1l} + (d_M - d_m + 1) \sum_{r=1}^h \tilde{Q}_{1rl} + \mu \tilde{R}_{1l}, \\ \tilde{Y}_{113} &= -\chi P_{3l} + (d_M - d_m + 1) \sum_{r=1}^h \tilde{Q}_{2rl} + \mu \tilde{R}_{2l}, \\ \tilde{Y}_{161} &= \mathcal{A}^T Y_1 + \mathcal{C}_i^T \Pi_{\lambda_1}^T \Pi_l^T \hat{H}_{Fij}^T + \mathcal{C}_i^T \Pi_{\lambda_2}^T \Pi_l^T \hat{H}_{Fij}^T, \\ \tilde{Y}_{162} &= \mathcal{A}^T Y_3 + \mathcal{C}_i^T \Pi_{\lambda_1}^T \Pi_l^T \hat{H}_{Fij}^T + \mathcal{C}_i^T \Pi_{\lambda_2}^T \Pi_l^T \hat{H}_{Fij}^T, \\ \tilde{Y}_{171} &= \theta_{\lambda_{1i}} \mathcal{C}_i^T \phi_l \Pi_l^T \hat{H}_{Fij}^T, \quad \tilde{Y}_{172} = \theta_{\lambda_{1i}} \mathcal{C}_i^T \phi_l \Pi_l^T \hat{H}_{Fij}^T, \quad \tilde{Y}_{181} = \theta_{\lambda_{2i}} \mathcal{C}_i^T \phi_l \Pi_l^T \hat{H}_{Fij}^T, \\ \tilde{Y}_{182} &= \theta_{\lambda_{2i}} \mathcal{C}_i^T \phi_l \Pi_l^T \hat{H}_{Fij}^T, \quad \tilde{Y}_{221} = -\text{diag}\{\tilde{Q}_{11l}, \dots, \tilde{Q}_{1hl}\}, \quad \tilde{Y}_{222} = -\text{diag}\{\tilde{Q}_{21l}, \dots, \tilde{Q}_{2hl}\}, \\ \tilde{Y}_{261} &= \tilde{\beta}_h \mathcal{A}_{d1}^T Y_1^T + \theta_{\beta_h} \mathcal{A}_{d1}^T Y_1^T, \quad \tilde{Y}_{262} = \tilde{\beta}_h \mathcal{A}_{d1}^T Y_3^T + \theta_{\beta_h} \mathcal{A}_{d1}^T Y_3^T, \quad \tilde{Y}_{361} = \tilde{\xi} \mathcal{A}_{d2}^T Y_1^T + \theta_{\xi} \mathcal{A}_{d2}^T Y_1^T, \\ \tilde{Y}_{362} &= \tilde{\xi} \mathcal{A}_{d2}^T Y_3^T + \theta_{\xi} \mathcal{A}_{d2}^T Y_3^T, \quad \tilde{Y}_{461} = \mathcal{B}^T Y_1^T + \mathcal{D}_i^T \Pi_l^T \hat{H}_{Fij}^T, \quad \tilde{Y}_{462} = \mathcal{B}^T Y_3^T + \mathcal{D}_i^T \Pi_l^T \hat{H}_{Fij}^T, \\ \tilde{Y}_{561} &= \Pi_{\lambda_2}^T \Pi_l^T \hat{H}_{Fij}^T, \quad \tilde{Y}_{562} = \Pi_{\lambda_2}^T \Pi_l^T \hat{H}_{Fij}^T, \quad \tilde{Y}_{581} = \phi_l^T \Pi_l \hat{H}_{Fij}^T, \quad \tilde{Y}_{582} = \phi_l^T \Pi_l \hat{H}_{Fij}^T, \\ \tilde{\Gamma}_1 &= \tilde{P}_{1l} - Y_1^T - Y_1, \quad \tilde{\Gamma}_2 = \tilde{P}_{2l} - Y_3^T - Y_2, \quad \tilde{\Gamma}_3 = \tilde{P}_{3l} - Y_2^T - Y_2, \\ \tilde{N}_{1ij} &= [0 \ N_{1ij} \ \underbrace{0 \dots 0}_{13} \ 0], \quad \tilde{M}_1 = [\underbrace{0 \dots 0}_8 \ M^T Y_2^T \ M^T Y_2^T \ \underbrace{0 \dots 0}_5], \\ \tilde{N}_{2ij} &= [N_1 \ \underbrace{0 \dots 0}_5 \ N_7 \ N_8 \ \underbrace{0 \dots 0}_7], \\ \tilde{M}_2 &= [\underbrace{0 \dots 0}_8 \ M^T Y_2^T \ M^T Y_2^T \ M^T Y_2^T \ M^T Y_2^T \ M^T Y_2^T \ M^T Y_2^T \ M^T Y_2^T \ 0], \\ N_1 &= \mathcal{C}_i^T \Pi_{\lambda_1}^T \Pi_l^T N_{2ij}^T + \mathcal{C}_i^T \Pi_{\lambda_2}^T \Pi_l^T N_{2ij}^T + \theta_{\lambda_{1i}} \mathcal{C}_i^T \phi_l^T \Pi_l^T N_{2ij}^T + \theta_{\lambda_{2i}} \mathcal{C}_i^T \phi_l^T \Pi_l^T N_{2ij}^T, \\ N_7 &= \mathcal{D}_i^T \Pi_l^T N_{2ij}^T \quad \text{and} \quad N_8 = \Pi_{\lambda_{2i}}^T \Pi_l^T N_{2ij}^T. \end{aligned}$$

Moreover, the gain matrices of the distributive non-fragile filter (8) are given as

$$\hat{K}_{ij} = Y_2^{-1} \hat{K}_{Fij}, \hat{H}_{ij} = Y_2^{-1} \hat{H}_{Fij} \text{ and } L_{ii} = L_{Fii}.$$

Proof For convenience and to accomplish the required results, the matrices are defined as follows: $P_l = \begin{bmatrix} \bar{P}_{1l} & \bar{P}_{2l} \\ \bar{P}_{2l}^T & \bar{P}_{3l} \end{bmatrix}$, $Y = \begin{bmatrix} Y_1 & Y_2 \\ Y_3 & Y_2 \end{bmatrix}$, $R_l = \text{diag}\{\bar{R}_{1l}, \bar{R}_{2l}\}$ and $Q_{rl} = \text{diag}\{\bar{Q}_{1rl}, \bar{Q}_{2rl}\}$ ($r = 1, 2, \dots, h$). Further, let $\hat{K}_{ij} = \hat{K}_{Fij}$, $\hat{H}_{ij} = \hat{H}_{Fij}$ and $L_{ii} = L_{Fii}$. Using the above given partition matrices P_l , \bar{R}_l , Q_{rl} , Y and applying Lemma 3 in [10] to the matrix inequality (11) together with parametric uncertainties, we have

$$\hat{\Upsilon} = [\bar{\Upsilon}]_{9 \times 9} + \epsilon_1 \bar{N}_{1ij}^T \Delta(k) \bar{M}_1 + \epsilon_2 \bar{M}_1^T \Delta(k) \bar{N}_{2ij}, \tag{34}$$

where the elements of $[\bar{\Upsilon}]_{9 \times 9}$, N_{1ij} , N_{2ij} , \bar{M}_1 and \bar{M}_2 are defined in Theorem 2. On the other hand, by using Lemma 3 in [30], the matrix term in (34) can be expressed as

$$\hat{\Upsilon} = [\bar{\Upsilon}]_{9 \times 9} + \epsilon_1 \bar{N}_{1ij}^T \bar{N}_{1ij} + \epsilon_1 \bar{M}_1 \bar{M}_1^T + \epsilon_2 \bar{N}_{2ij}^T \bar{N}_{2ij} + \epsilon_2 \bar{M}_2 \bar{M}_2^T. \tag{35}$$

The expression in (35) can be shown to be equivalent to the matrix terms in (33). Hence, if the LMIs in (33) together with (12) hold, then the augmented filtering error system (9) is stochastically finite-time bounded with $(\mathcal{X}, \mathcal{Y}, \mathcal{Z}) - \gamma$ dissipative performance index subject to $(\sigma_1, \sigma_2, \mathbb{N}, \gamma, \mathcal{J}, \varphi)$. This completes the proof. \square

Next, if we assume the system (1) without distributed time-varying delay and infinitely distributed delay, then the augmented filtering error system (8) can be modified as follows:

$$\begin{aligned} \eta(k) &= \tilde{\mathcal{A}}\eta(k) + \tilde{\mathcal{D}}\tilde{w}(k) + \tilde{\mathcal{E}}v(k) + \mathcal{W}_1\eta(k) + \mathcal{W}_2\eta(k) + \mathcal{W}_E v(k), \\ e(k) &= \tilde{L}\eta(k), \\ y_i(k) &= \tilde{\mathcal{C}}_i\eta(k). \end{aligned} \tag{36}$$

Corollary 1 Let $\bar{\lambda}_{1i}$, $\bar{\lambda}_{2i}$, χ , $\theta_{\bar{\lambda}_{ci}}$ ($c = 1, 2$) be known positive scalars and $\mathcal{X} \leq 0$, \mathcal{Y} , $\mathcal{Z} = \mathcal{Z}^T$, $\mathcal{J} \geq 0$ be known constant matrices. The augmented filtering error system (9) is stochastically finite-time bounded with $(\mathcal{X}, \mathcal{Y}, \mathcal{Z}) - \gamma$ dissipative performance index subject to $(\sigma_1, \sigma_2, \mathbb{N}, \gamma, \mathcal{J}, \varphi)$ if there exist positive definite matrices \bar{P}_{1l} , \bar{P}_{2l} , \bar{P}_{3l} , any matrices Y_1, Y_2, Y_3 and positive scalars α_1, α_2 , such that the below given LMIs hold for every $l = 1, 2 \dots n_{2i} \times n_{2i} \in \Phi$:

$$\begin{bmatrix} [\Phi]_{7 \times 7} & \epsilon_1 \bar{N}_{1ij}^T & \bar{M}_1 & \epsilon_2 \bar{N}_{2ij}^T & \bar{M}_2 \\ * & -\epsilon_1 & 0 & 0 & 0 \\ * & * & -\epsilon_1 & 0 & 0 \\ * & * & * & -\epsilon_2 & 0 \\ * & * & * & * & -\epsilon_2 \end{bmatrix} < 0, \tag{37}$$

$$\alpha_2 \sigma_1 + \alpha_{\mathcal{W}} \varphi < \sigma_2 \alpha_1 \chi^{-k}, \tag{38}$$

$$\alpha_1 \leq P_l \leq \alpha_2, \tag{39}$$

where

$$\begin{aligned} \Phi_{11} &= \begin{bmatrix} -\chi P_{1l} & -\chi P_{2l} \\ * & -\chi P_{3l} \end{bmatrix}, \quad \Phi_{12} = \begin{bmatrix} -\mathcal{L}^T \mathcal{Y} \\ \mathcal{L}_{Fii}^T \mathcal{Y} \end{bmatrix}, \quad \Phi_{14} = \begin{bmatrix} \Phi_{141} & \Phi_{142} \\ \hat{K}_{Fij}^T & \hat{K}_{Fij}^T \end{bmatrix}, \quad \Phi_{15} = \begin{bmatrix} \Phi_{151} & \Phi_{152} \\ 0 & 0 \end{bmatrix}, \\ \Phi_{16} &= \begin{bmatrix} \Phi_{161} & \Phi_{162} \\ 0 & 0 \end{bmatrix}, \quad \Phi_{17} = \begin{bmatrix} -\mathcal{L}^T \sqrt{-\mathcal{X}} \\ \mathcal{L}_{Fii}^T \sqrt{-\mathcal{X}} \end{bmatrix}, \quad \Phi_{22} = -\mathcal{L} + \gamma I, \quad \Phi_{24} = [\Phi_{241} \quad \Phi_{242}], \\ \Phi_{33} &= -\frac{\mathcal{M}_\delta}{\Gamma_\delta} I, \quad \Phi_{34} = \begin{bmatrix} \Phi_{341} \\ \Phi_{342} \end{bmatrix}^T, \quad \Phi_{36} = \begin{bmatrix} \Phi_{361} \\ \Phi_{362} \end{bmatrix}^T, \quad \Phi_{44} = \begin{bmatrix} \hat{\Phi}_1 & \hat{\Phi}_2 \\ * & \hat{\Phi}_3 \end{bmatrix}, \quad \Phi_{55} = \begin{bmatrix} \hat{\Phi}_1 & \hat{\Phi}_2 \\ * & \hat{\Phi}_3 \end{bmatrix}, \\ \Phi_{66} &= \begin{bmatrix} \hat{\Phi}_1 & \hat{\Phi}_2 \\ * & \hat{\Phi}_3 \end{bmatrix}, \quad \Phi_{77} = -I, \quad \Phi_{141} = \mathcal{A}^T Y_1 + \mathcal{C}_i^T \Pi_{\lambda_1}^T \Pi_l^T \hat{H}_{Fij}^T + \mathcal{C}_i^T \Pi_{\lambda_2}^T \Pi_l^T \hat{H}_{Fij}^T, \\ \Phi_{142} &= \mathcal{A}^T Y_3 + \mathcal{C}_i^T \Pi_{\lambda_1}^T \Pi_l^T \hat{H}_{Fij}^T + \mathcal{C}_i^T \Pi_{\lambda_2}^T \Pi_l^T \hat{H}_{Fij}^T, \quad \Phi_{151} = \theta_{\lambda_{1i}} \mathcal{C}_i^T \phi_l^T \Pi_l^T \hat{H}_{Fij}^T, \\ \tilde{\Upsilon}_{152} &= \theta_{\lambda_{1i}} \mathcal{C}_i^T \phi_l^T \Pi_l^T \hat{H}_{Fij}^T, \quad \Phi_{161} = \theta_{\lambda_{2i}} \mathcal{C}_i^T \phi_l \Pi_l^T \hat{H}_{Fij}^T, \quad \Phi_{162} = \theta_{\lambda_{2i}} \mathcal{C}_i^T \phi_l^T \Pi_l \hat{H}_{Fij}^T, \\ \Phi_{241} &= \mathcal{B}^T Y_1^T + \mathcal{D}_i^T \Pi_l^T \hat{H}_{Fij}^T, \quad \Phi_{242} = \mathcal{B}^T Y_3^T + \mathcal{D}_i^T \Pi_l^T \hat{H}_{Fij}^T, \quad \Phi_{341} = \Pi_{\lambda_2}^T \Pi_l^T \hat{H}_{Fij}^T, \\ \Phi_{342} &= \Pi_{\lambda_2}^T \Pi_l^T \hat{H}_{Fij}^T, \quad \Phi_{361} = \phi_l^T \Pi_l \hat{H}_{Fij}^T, \quad \Phi_{362} = \phi_l^T \Pi_l^T \hat{H}_{Fij}^T, \quad \hat{\Phi}_1 = \bar{P}_{1l} - Y_1^T - Y_1, \\ \hat{\Phi}_2 &= \bar{P}_{2l} - Y_3^T - Y_2, \quad \hat{\Phi}_3 = \bar{P}_{3l} - Y_2^T - Y_2, \quad \bar{N}_{1ij} = [0 \quad N_{1ij} \quad \underbrace{0 \cdots 0}_9], \\ \bar{M}_1 &= [\underbrace{0 \cdots 0}_4 \quad M^T Y_2^T \quad M^T Y_2^T \quad \underbrace{0 \cdots 0}_5], \quad \bar{N}_{2ij} = [N_1 \quad 0 \quad N_3 \quad N_4 \quad \underbrace{0 \cdots 0}_7], \\ \bar{M}_2 &= [\underbrace{0 \cdots 0}_4 \quad M^T Y_2^T \quad M^T Y_2^T \quad M^T Y_2^T \quad M^T Y_2^T \quad M^T Y_2^T \quad M^T Y_2^T \quad 0], \\ N_1 &= \mathcal{C}_i^T \Pi_{\lambda_1}^T \Pi_l^T N_{2ij}^T + \mathcal{C}_i^T \Pi_{\lambda_2}^T \Pi_l^T N_{2ij}^T + \theta_{\lambda_{1i}} \mathcal{C}_i^T \phi_l^T \Pi_l^T N_{2ij}^T + \theta_{\lambda_{2i}} \mathcal{C}_i^T \phi_l^T \Pi_l^T N_{2ij}^T, \\ N_3 &= \mathcal{D}_i^T \Pi_l^T N_{2ij}^T, \quad N_4 = \Pi_{\lambda_{2i}}^T \Pi_l^T N_{2ij}^T, \end{aligned}$$

Moreover, the gain matrices of the distributive non-fragile filter (8) are given as

$$\hat{K}_{ij} = Y_2^{-1} \hat{K}_{Fij}, \quad \hat{H}_{ij} = Y_2^{-1} \hat{H}_{Fij} \text{ and } L_{ii} = L_{Fii}.$$

Proof The proof of this corollary is similar to Theorem 2 and hence it is neglected. \square

Remark 2 This paper proposes a new set of conditions for the considered complex system (1) by using distributive filtering techniques. The main advantage of the proposed filter technique is that it can ensure the desired result even in the presence of packet losses and uncertainties in the filter components. On the other hand, dissipative performance is a more generalized and effective technique in designing the filter for linear and nonlinear systems. In addition, the addressed system (1) incorporates some reality factors such as uncertainty, stochastic distributed time delays and packet losses, so that the system model addressed is comprehensive and the results presented in this paper are more applicable in practice.

4 Numerical Simulation

In this section, we illustrate two examples to show the validity of the proposed theoretical results. Specifically, the first example is presented to demonstrate the stochastic finite-time boundedness with prescribed performance index for the augmented filtering error system (9) with distributed time-varying delay, infinitely distributed time delay, dynamic quantizer and energy constraints. Furthermore, the remaining example is provided to prove the efficiency of the proposed results for system (36).

Example 1 In this example, the sensor network is presented in terms of direct graph $\mathbb{G} = (\mathbb{V}, \mathbb{E}, \mathbb{A})$, with $\mathbb{V} = \{1, 2\}$ and $\mathbb{E} = \{(1, 1), (1, 2), (2, 2)\}$, where \mathbb{V} and \mathbb{E} are the set of nodes and edges of the graph, respectively. Moreover, we consider the adjacency matrix as

$$\mathbb{A} = \begin{bmatrix} 1 & 1 \\ 0 & 1 \end{bmatrix}.$$

Let us assume the complex system (1) with corresponding matrices as

$$A = \begin{bmatrix} -0.023 & 0.002 & 0.014 \\ 0.026 & 0.024 & 0.04 \\ 0.28 & 0.22 & 0.08 \end{bmatrix}, \quad A_{d1} = \begin{bmatrix} -0.003 & 0.001 & 0.003 \\ 0.002 & -0.003 & 0.004 \\ 0.002 & 0.006 & -0.001 \end{bmatrix},$$

$$A_{d2} = \begin{bmatrix} -0.001 & 0.001 & 0.06 \\ 0.001 & -0.001 & 0.003 \\ 0.001 & 0.004 & -0.006 \end{bmatrix}, \quad B = [0.8 \ 0.5 \ 0.2]^T \text{ and } L = [1 \ 1 \ 0].$$

The parametric uncertainties are taken as

$$M = [0.01 \ 0.07 \ 0.03]^T, \quad N_{a11} = [0.2 \ 0.8 \ 0.1], \quad N_{a12} = [0.7 \ 0.4 \ 0.2],$$

$$N_{a21} = [0.3 \ 0.6 \ 0.9], \quad N_{a22} = [0.2 \ 0.5 \ 0.6], \quad N_{b11} = 0.03, \quad N_{b12} = 0.07,$$

$$N_{b21} = 0.06 \text{ and } N_{b22} = 0.03.$$

Specifically, the measurement output of the i^{th} sensor node with $i, j = 1, 2$ is described as in (6) and the parameter values are chosen as

$$C_1 = [1 \ 0 \ 1], \quad C_2 = [0 \ 1 \ 1], \quad D_1 = 0.5 \text{ and } D_2 = 0.2.$$

Next, we assume that the distributed time delay satisfies $1 \leq d_r(k) \leq 4$, where $r = 1, 2$ with $d_1(k) = 1.2 + 0.2 \cos(k)$ and $d_2(k) = 2 + 0.9 \sin(k)$. Further, the communication delay bound satisfies $1 \leq \tilde{\tau}_r(k) \leq 3$ ($r = 1, 2$) which occurs stochastically. Moreover, the parameters $\mathcal{M}_\delta = 10$ and $\Gamma_\delta = 2.1$ are the error bound and range of the dynamic quantizer, respectively. The occurrence probabilities for packet losses and dynamic quantization are taken for each sensor nodes. For the first and second sensor nodes, we choose $\bar{\lambda}_{11} = 0.2$, $\bar{\lambda}_{21} = 0.15$, $\bar{\lambda}_{12} = 0.6$ and $\bar{\lambda}_{22} = 0.15$.

The other parameters are chosen as $\chi = 1.1$, $\varrho = 2.5$, $\mathcal{X} = -0.5$, $\mathcal{Y} = 0.3$ and $\mathcal{Z} = 2.6$. Furthermore, the switching signal $\rho(k)$ can be taken periodically as

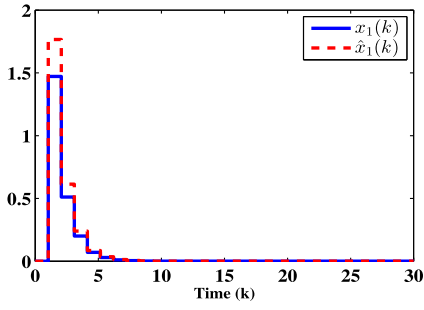
$$\rho(k) = \begin{cases} 1, & 1 \leq k \leq 15, \\ 2, & 15 \leq k \leq 30. \end{cases}$$

By solving the LMI constraints derived in Theorem 2 together with the above given parameters, we obtain the minimum value of γ as $\gamma = 0.9754$ and the filter gain matrices as

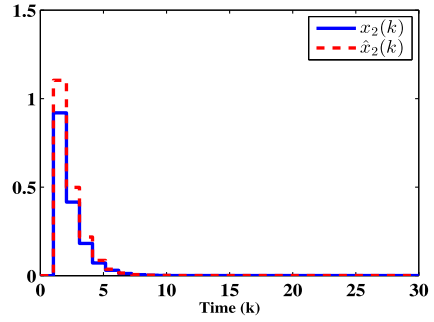
$$\begin{aligned} K_{11} &= \begin{bmatrix} 0.0098 & 0.0043 & -0.0017 \\ 0.0024 & 0.0010 & -0.0034 \\ 0.0018 & 0.0009 & -0.0003 \end{bmatrix}, & K_{12} &= \begin{bmatrix} -0.0118 & -0.0048 & 0.0016 \\ -0.0035 & -0.0012 & 0.0035 \\ -0.0021 & -0.0010 & 0.0003 \end{bmatrix}, \\ K_{22} &= \begin{bmatrix} 0.0337 & 0.0542 & -1.1035 \\ 0.0256 & 0.0471 & -0.3342 \\ -0.0015 & 0.0010 & -0.1205 \end{bmatrix}, & H_{11} &= \begin{bmatrix} -0.6010 \\ -0.3149 \\ -0.2269 \end{bmatrix}, & H_{12} &= \begin{bmatrix} -0.3385 \\ -0.3111 \\ -0.0268 \end{bmatrix}, \\ H_{22} &= \begin{bmatrix} -0.0020 \\ -0.0054 \\ -0.0024 \end{bmatrix}, & L_{11} &= [0.8890 \ 0.7778 \ 0.2675], \\ L_{22} &= [0.8939 \ 0.7802 \ 0.2540]. \end{aligned}$$

Let us set the initial conditions as $x(0) = x_f(0) = [0 \ 0]^T$ for the system and filter states. Moreover, we assume $\tilde{w}(k) = 4 \cos(k) \exp(-0.1k)$ to be the disturbance input, and from (16), we take $v(k) = \frac{\sqrt{2.5 \times 2.1}}{10} y(k)$. Further, with the above-mentioned values the simulation results for the considered system (1) are represented in Figs. 2, 3, 4, 5 and 6. Figure 2 shows the system states and their corresponding estimates. Eventually, the trajectories of the output $z(k)$ and its estimate $\hat{z}(k)$ are displayed in Fig. 3. Moreover, Fig. 4 displays the response of error system with and without quantization of the augmented filtering error system (9). To be more particular from Fig. 4, it is clear that the proposed filter works efficiently even in the presence of quantization. The switching signal throughout the simulation process is presented in 5. Furthermore, the time history of the filtering error system (9) is depicted in Fig. 6. Finally, Table 1 presents the calculated γ value for different upper bounds for various performances. Hence, it is evident from this example that the augmented filtering error system (9) is stochastically finite-time bounded with $(\mathcal{X}, \mathcal{Y}, \mathcal{Z}) - \gamma$ dissipative performance index subject to $(0.4, 20.4739, 30, 0.9754, I, 0.1)$ under the proposed distributive non-fragile filter design.

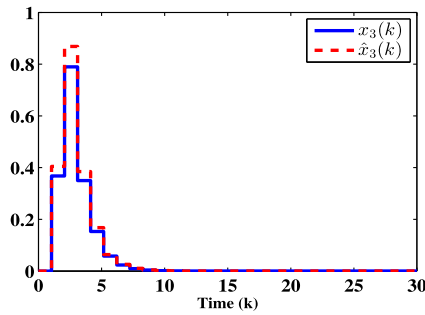
Example 2 In this example, a CSTR model as in [33] is considered to show the efficiency of proposed distributive filter design. The complete reaction is given as follows: cyclopentadiene (A) \rightarrow cyclopentanol (B) \rightarrow cyclopentanediol (C), and 2 cyclopentadiene (A) \rightarrow dicyclopentadiene (D). Also, the production of cyclopentanol (B) from cyclopentadiene (A) is considered. By assuming constant density and an ideal residence time distribution within the reactor, the balance equations can be described in the following form:



(a) Trajectories of $x_1(k)$ and $\hat{x}_1(k)$



(b) Trajectories of $x_2(k)$ and $\hat{x}_2(k)$



(c) Trajectories of $x_3(k)$ and $\hat{x}_3(k)$

Fig. 2 Responses of the states and their corresponding estimates

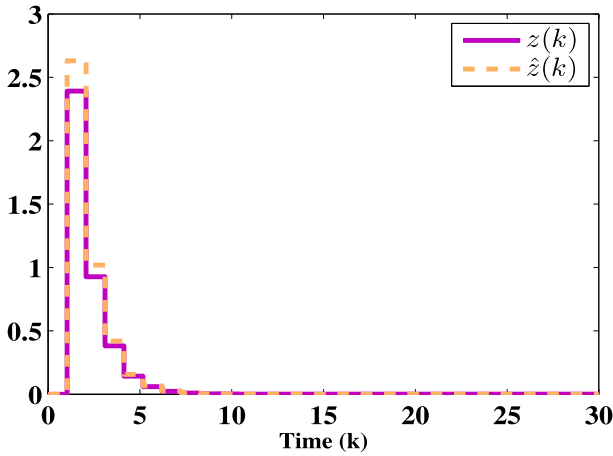


Fig. 3 Trajectories of $z(k)$ and $\hat{z}(k)$

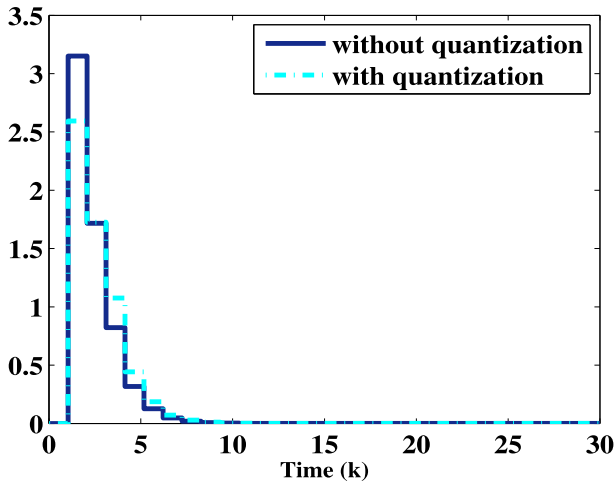


Fig. 4 Trajectories of error system (9)

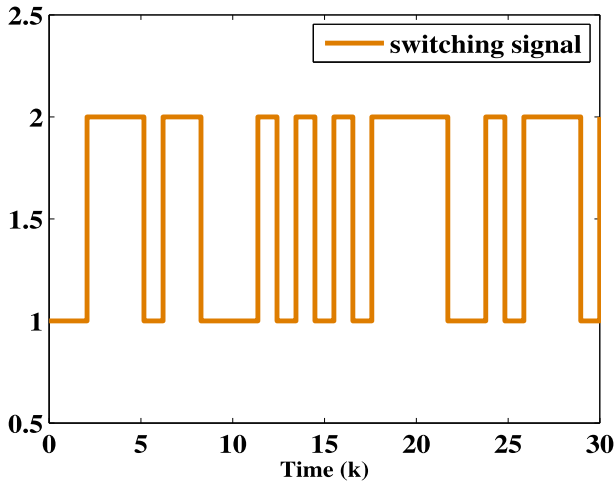


Fig. 5 Switching signal

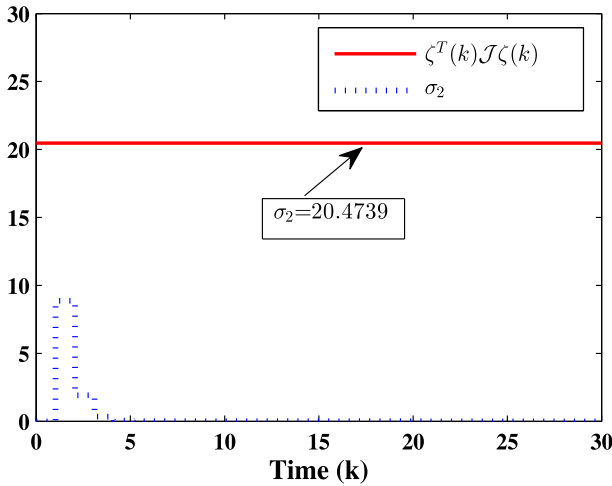


Fig. 6 Evolution of $x^T(k) \mathcal{J} x(k)$

Table 1 Calculated γ for various values of d_M

d_M	2	3	4
Dissipative case ($\chi = 1.1$)	0.5844	0.7826	0.9754
H_∞ case ($\chi = 1.3$)	0.9168	1.2153	1.3473
Mixed H_∞ and passivity case ($\chi = 1.4$)	1.1761	1.3267	1.5892

$$\begin{aligned}
 \frac{dC_A}{dt} &= \frac{\dot{V}}{V_R} (C_{A0} - C_A) - k_1 C_A - k_3 C_A^2, \\
 \frac{dC_B}{dt} &= -\frac{\dot{V}}{V_R} C_B + k_1 C_A - k_2 C_B, \\
 \frac{d\vartheta}{dt} &= \frac{\dot{V}}{V_R} (\vartheta_0 - \vartheta) + \frac{k_w A_R}{\zeta C_p V_R} (\vartheta_K - \vartheta) \\
 &\quad - \frac{k_1 C_A \Delta H_R^{AB} + k_2 C_B \Delta H_R^{BC} + k_3 C_A^2 \Delta H_R^{AD}}{\zeta C_p}, \tag{40}
 \end{aligned}$$

where C_A denotes the concentration of educt A; C_B represents the concentration of the desired product B within the reactor; and ϑ is the reactor temperature. The rate components k_1 , k_2 and k_3 depend exponentially on the react temperature ϑ via Arrhenius law given by $k_i(\vartheta) = k_{0i} \exp(\frac{-E_{Ai}}{R\vartheta})$ ($i = 1, 2, 3$). Let us assume that the first and second rate components are equal for the reaction system, that is $k_1 = k_2$. Further, the values for model parameters are defined as $k_{01} = k_{02} = 1.287 \times 10^{12} \text{ h}^{-1}$, $k_{03} = 9.043 \times 10^9 \text{ l/mol/h}^{-1}$, $E_{A1}/R = E_{A2}/R = 9758.3 \text{ K}$, $E_{A3}/R = 8560.0 \text{ K}$, $\Delta H_R^{AB} = 4.2 \text{ kJ/mol}$, $\Delta H_R^{BC} = -11 \text{ kJ/mol}$, $\Delta H_R^{AD} = -41.85 \text{ kJ/mol}$, $C_p = 3.01 \text{ kJ/kgK}$, $A_R = 0.215 \text{ m}^2$, $V = 10.01$, $\vartheta_0 = 403.15 \text{ K}$, $k_w = 4032 \text{ kJ/hm}^2 \text{ K}$.

Now, linearizing the balance equations (40) at the operating point, we can obtain the state-space model in the following form:

$$\dot{x}(t) = A_p x(t) + B_p u(t), \quad (41)$$

where $x = \begin{bmatrix} x_1 \\ x_2 \\ x_3 \end{bmatrix} = \begin{bmatrix} C_A - C_{As} \\ C_B - C_{Bs} \\ \vartheta - \vartheta_s \end{bmatrix}$, $u = \begin{bmatrix} u_1 \\ u_2 \end{bmatrix} = \begin{bmatrix} \dot{V} - \dot{V}_s \\ C_{A0} - C_{A0s} \end{bmatrix}$, and the matrices A_p and B_p are given by

$$A_p = \begin{bmatrix} -86.0962 & 0 & 4.2077 \\ 50.6146 & -69.4446 & -0.9974 \\ 172.2263 & 197.9985 & -65.5149 \end{bmatrix} \quad \text{and} \quad B_p = \begin{bmatrix} 0.3861 & 18.83 \\ -0.0899 & 0 \\ -0.4136 & 0 \end{bmatrix}.$$

The steady-state values of the main operating point of the reactor are given by $C_{As} = 1.235 \text{ mol/l}$, $C_{Bs} = 0.9 \text{ mol/l}$, $\vartheta_s = 407.29 \text{ K}$, $\dot{V}/V_R = 18.83 \text{ h}^{-1}$, $C_{A0s} = 5.1 \text{ mol/l}$. It should be noted that the control input can be treated as the unknown input signal in the state estimation problem. According to this point, the discrete-time state representation of (41) with the sampling period $T_0 = 1 \text{ min}$ can be represented by the following equation:

$$x(k+1) = Ax(k) + B\tilde{w}(k), \quad (42)$$

where

$$A = \begin{bmatrix} 0.2747 & 0.0345 & 0.0206 \\ 0.2323 & 0.3152 & 0.0033 \\ 1.2566 & 1.1042 & 0.3671 \end{bmatrix} \quad \text{and} \quad B = \begin{bmatrix} 1 \\ 1 \\ 1 \end{bmatrix}.$$

Here, we have considered two sensor nodes for the combined measurements (6) and are taken as

$$C_1 = [1 \ 0 \ 0], \quad C_2 = [0 \ 0 \ 1], \quad D_1 = 0.3, \quad D_2 = 0.2 \quad \text{and} \quad L = [0 \ 1 \ 0].$$

Suppose the disturbance variation occurs in the range which lies between $[-1, 1]$ and also, the missing measurements are taken as $\bar{\lambda}_{11} = 0.15$, $\bar{\lambda}_{21} = 0.35$, $\bar{\lambda}_{12} = 0.48$ and $\bar{\lambda}_{22} = 0.2$. Moreover, the additional parameter values are chosen as $\chi = 1$, $\bar{\beta}_1 = 0.547$, $\bar{\beta}_2 = 0.5$, $\bar{\xi} = 0.22$, $\varrho = 1.5$, $\mathcal{X} = -0.01$, $\mathcal{Y} = 1.4$, $\mathcal{Z} = 3.6$ and other parameter values are same as in Example 1. Then, by solving the LMIs in Corollary 1 and using the above given values, we obtain minimum $\gamma = 1.4121$ and the gain matrices as follows:

$$K_{11} = \begin{bmatrix} -0.3157 & -0.0199 & 0.0611 \\ -0.2953 & -0.0178 & 0.0566 \\ -0.1736 & -0.0117 & 0.0320 \end{bmatrix}, \quad K_{12} = \begin{bmatrix} 0.3082 & 0.0110 & -0.0336 \\ 0.2853 & 0.0112 & -0.0324 \\ 0.1673 & 0.0062 & -0.0228 \end{bmatrix},$$

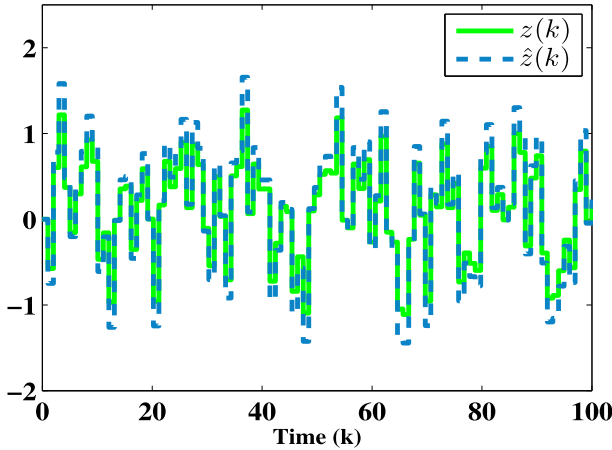


Fig. 7 Trajectories of $z(k)$ and $\hat{z}(k)$

$$\begin{aligned}
 K_{22} &= \begin{bmatrix} -0.0197 & -0.0139 & -0.0158 \\ -0.0200 & -0.0126 & -0.0145 \\ -0.0122 & -0.0087 & -0.0101 \end{bmatrix}, \quad H_{11} = \begin{bmatrix} -4.3194 & 0 \\ -3.8751 & 0 \\ -2.1170 & 0 \end{bmatrix}, \\
 H_{21} &= \begin{bmatrix} -3.2841 & -0.2437 \\ -3.0214 & -0.1788 \\ -1.7366 & -0.0344 \end{bmatrix}, \quad H_{22} = \begin{bmatrix} -0.2439 & -0.2439 \\ -0.1789 & -0.1789 \\ -0.0345 & -0.0345 \end{bmatrix}, \\
 L_{11} &= \begin{bmatrix} 0.5394 \\ -1.5832 \\ 1.3528 \end{bmatrix}^T, \quad L_{22} = \begin{bmatrix} 0.5533 \\ -1.6499 \\ 1.4737 \end{bmatrix}^T.
 \end{aligned}$$

The initial conditions for the state and filter are chosen as $x(0) = [0 \ 0]^T$ and $x_f(0) = [0 \ 0]^T$, respectively. With the aid of initial conditions and aforementioned parameters, the simulation results are presented in Figs. 7, 8, 9 and 10. In particular, the trajectories of the output signal $z(k)$ and its estimation $\hat{z}(k)$ are displayed in Fig. 7. The error responses of the augmented filtering error system (36) are plotted in Fig. 8. The switching signal at each time instant is depicted in 9. Further, Fig. 10 depicts the time evaluation of $\zeta^T(k) \mathcal{J} \zeta(k)$ with optimum bound value σ_2 . In particular, it is clear that the state trajectories do not exceed the maximum allowable bound value σ_2 . Moreover, Table 2 shows the maximum allowable bound value of σ_2 for different values of σ_1 . Finally, Table 3 displays the minimum γ value for different methods, and also, it is evident that Corollary 1 is less conservative than Theorem 2 of Zhang et al. [33]. Hence, it can be concluded from this example that the augmented filtering error system in (36) is stochastically finite-time bounded with $(\mathcal{X}, \mathcal{Y}, \mathcal{L}) - \gamma$ dissipative performance subject to $(0.2, 34.4040, 100, 1.4121, I, 0.05)$.

Example 3 Now, we will apply the conditions derived in Corollary 1 to deal with the distributive filter problem for a quarter-car suspension system as in [34]. Moreover,

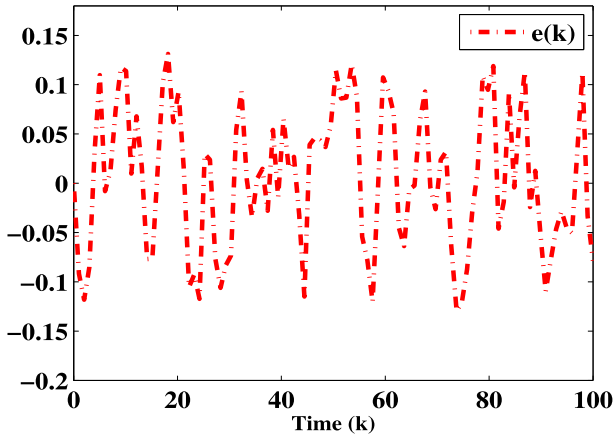


Fig. 8 Response of error system (36)

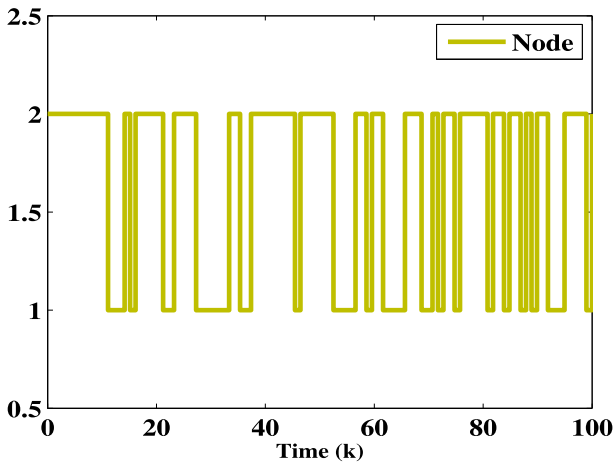


Fig. 9 Switching signal

the corresponding parametric values are borrowed from Zhang et al. [34], which are given as follows:

$$A = \begin{bmatrix} 0.5610 & 0.7804 & 0.0447 & 0.0037 \\ 0.3297 & -0.0001 & 0.0436 & 0.0014 \\ -1.9618 & -4.5284 & 0.7529 & 0.0274 \\ -1.3703 & -1.2849 & 0.2335 & -0.2335 \end{bmatrix}, \quad B = \begin{bmatrix} -0.0024 \\ -0.0023 \\ 0.0110 \\ 0.0503 \end{bmatrix}, \quad \text{and } L = [0 \ 0 \ 1 \ 0].$$

Further, the uncertain parametric matrix values are assumed as

$$M = [0.06 \ 0.03 \ 0.06 \ 0.02]^T, \quad N_{a11} = [0.01 \ 0.04 \ 0.01 \ 0.03], \\ N_{a12} = [0.02 \ 0.05 \ 0.03 \ 0.01], \quad N_{a22} = [0.07 \ 0.04 \ 0.02 \ 0.01],$$

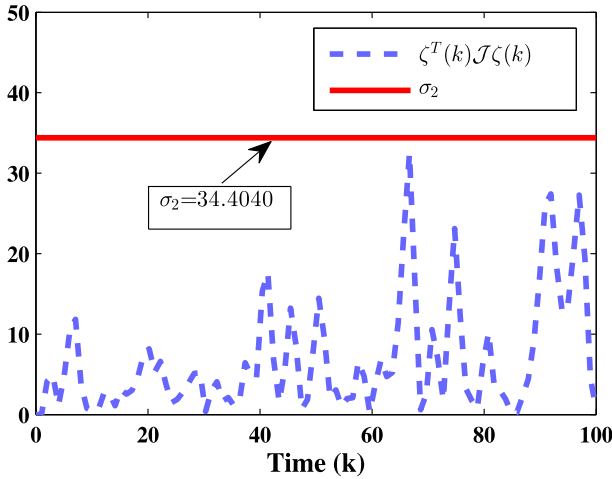


Fig. 10 Evolution of $\zeta^T(k)J\zeta(k)$

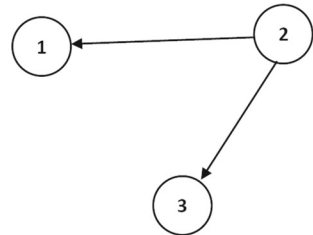
Table 2 Maximum σ_2 bound for various σ_1 values

σ_1	0.2	0.4	0.6	0.8	1
σ_2	34.4040	35.1248	35.8765	36.59874	37.1549

Table 3 Comparison of minimum γ by various methods

Methods	γ
Corollary 1	1.4121
[33]	1.9069

Fig. 11 Topological structure of sensor network



$$N_{a32} = [0.06 \ 0.01 \ 0.04 \ 0.02], \quad N_{a33} = [0.05 \ 0.04 \ 0.03 \ 0.02],$$

$$N_{b11} = 0.02, \quad N_{b12} = 0.03, \quad N_{b22} = 0.05, \quad N_{b32} = 0.07 \quad \text{and} \quad N_{b33} = 0.02.$$

In this example, we assume that the sensor with three nodes and the corresponding graph topologies are displayed in Fig. 11. In particular, the measurement output in (6) is assumed with three sensor nodes and the parametric values are taken as

$$C_1 = \begin{bmatrix} 1 & 0 & 0 & 0 \\ 0 & 1 & 0 & 0 \end{bmatrix}, \quad C_2 = [0 \ 0 \ 0 \ 1], \quad C_3 = [0 \ 0 \ 0 \ 1],$$

$$D_1 = [0.11 \ 0.2], \quad D_2 = 0.02 \quad \text{and} \quad D_3 = 0.03.$$

Here, only one node of Y_i is selected at each time instant for transmission and for three nodes $\Pi_{\rho_i(k)}$ ($i = 1, 2, 3$) is assumed as $\Pi_{\rho_i(k)} \in \{[10], [01]\}$, $\Pi_{\rho_2(k)} = 1$ and $\Pi_{\rho_3(k)} = 1$. Moreover, the error bound and the range of the dynamic quantizer parametric values are $\mathcal{M}_\delta = 10$ and $\Gamma_\delta = 1.5$, respectively. The probability of packet loss encountered for each sensor node is chosen as $\alpha_{11}^- = 0.35$, $\alpha_{12}^- = 0.4$, $\alpha_{13}^- = 0.6$, $\alpha_{21}^- = 0.2$, $\alpha_{22}^- = 0.5$ and $\alpha_{23}^- = 0.75$. The remaining parametric values are taken same as in Example 2. By using aforementioned values and solving the derived LMIs in Corollary 1, we obtain $\gamma = 0.3358$ and the gain matrices are as follows:

$$\begin{aligned}
 K_{11} &= \begin{bmatrix} -0.5847 & -0.5461 & -0.8705 & -0.4925 \\ -0.5893 & 0.5495 & -0.7181 & -0.4339 \\ 0.3271 & -0.2972 & -0.2342 & -0.1025 \\ -0.3312 & -0.3140 & -0.1574 & -0.1932 \end{bmatrix}, \\
 K_{12} &= \begin{bmatrix} -0.5485 & 0.54019 & -0.79291 & -0.5553 \\ -0.5649 & 0.5460 & -0.7216 & -0.4726 \\ 0.39105 & -0.3099 & 0.2322 & 0.9003 \\ 0.3383 & -0.3153 & -0.1592 & -0.1946 \end{bmatrix}, \\
 K_{22} &= \begin{bmatrix} 0.1079 & 0.26546 & -0.3538 & 0.3163 \\ 0.1286 & 0.18047 & -0.1279 & 0.8635 \\ 0.4378 & 0.1422 & 0.2781 & -0.2212 \\ 0.3276 & -0.2604 & -0.6663 & -0.4616 \end{bmatrix}, \\
 K_{32} &= \begin{bmatrix} 0.1829 & 0.2554 & -0.4062 & 0.2803 \\ 0.2417 & 0.1268 & -0.1403 & 0.8194 \\ 0.3233 & -0.1775 & -0.3000 & -0.2170 \\ 0.3226 & -0.2501 & -0.3959 & -0.5026 \end{bmatrix}, \\
 K_{33} &= \begin{bmatrix} 0.1722 & 0.2296 & -0.3831 & 0.2572 \\ 0.2706 & -0.6602 & -0.1448 & 0.7833 \\ 0.1372 & -3.3003 & 0.3325 & -0.2123 \\ 0.2955 & -0.2272 & -0.4792 & -0.4831 \end{bmatrix}, \\
 H_{11} &= \begin{bmatrix} -0.4042 \\ -0.1532 \\ -0.1258 \\ -0.2017 \end{bmatrix}, \quad H_{12} = \begin{bmatrix} -0.4173 \\ -0.1738 \\ -0.1229 \\ -0.1938 \end{bmatrix}, \quad H_{22} = \begin{bmatrix} 0.0521 \\ -0.1324 \\ -0.3422 \\ -0.4163 \end{bmatrix}, \\
 H_{32} &= \begin{bmatrix} -0.4342 \\ -0.1193 \\ -0.3253 \\ -0.4252 \end{bmatrix}, \quad H_{33} = \begin{bmatrix} -0.4342 \\ -0.1193 \\ -0.3254 \\ -0.4254 \end{bmatrix}, \quad L_{11} = \begin{bmatrix} 3.6090 \\ -3.2170 \\ -4.6092 \\ -1.1311 \end{bmatrix}^T, \\
 L_{22} &= \begin{bmatrix} 5.4983 \\ -4.9722 \\ -8.0638 \\ -1.2694 \end{bmatrix}^T \quad \text{and} \quad L_{33} = \begin{bmatrix} 3.9953 \\ -3.5837 \\ -5.0567 \\ -1.1203 \end{bmatrix}^T.
 \end{aligned}$$

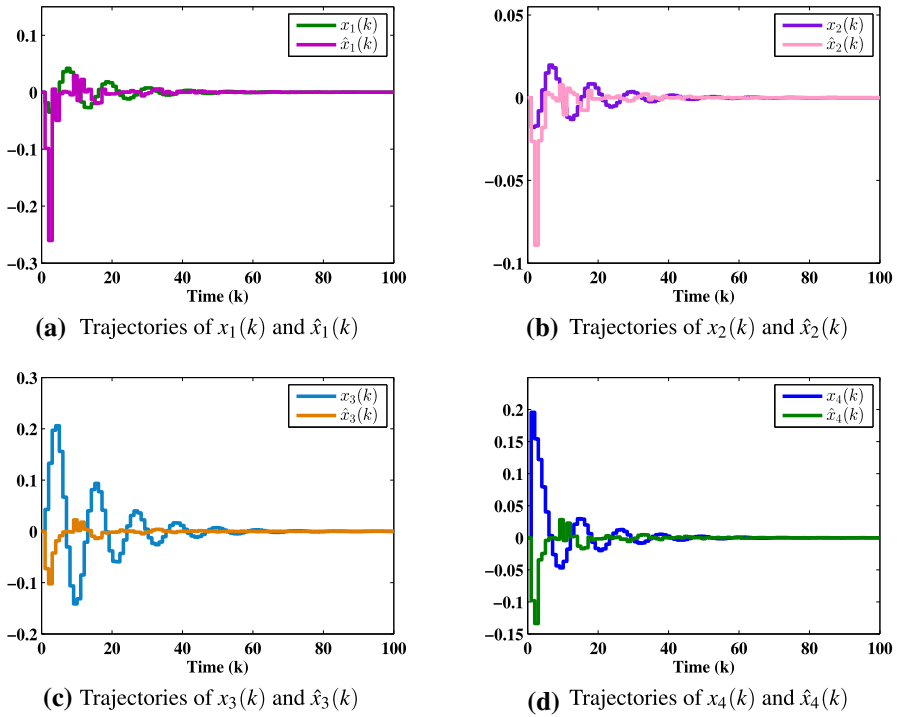


Fig. 12 Responses of the states and their corresponding estimates

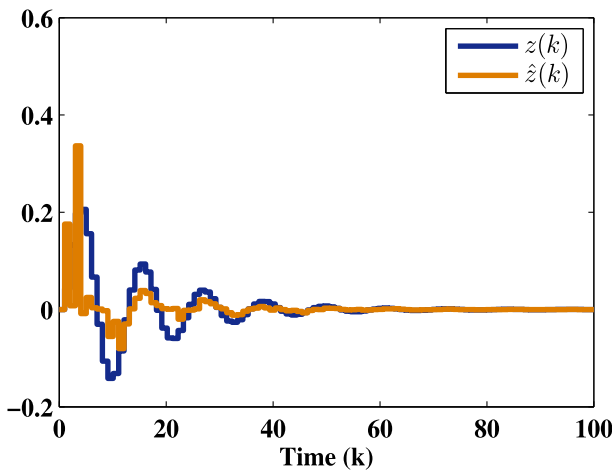


Fig. 13 Trajectories of $z(k)$ and $\hat{z}(k)$

The initial conditions for the system and filter state are taken as $x(0) = x_f(0) = [0 \ 0 \ 0 \ 0]^T$. Moreover, we assume $\tilde{w}(k) = 15 \exp(-0.7k) \sin(0.55k)$ to be the disturbance input. Further, with the aforementioned values the simulation results are displayed in Figs. 12, 13, 14, 15 and 16. The system states $x_b(k)$ and their correspond-

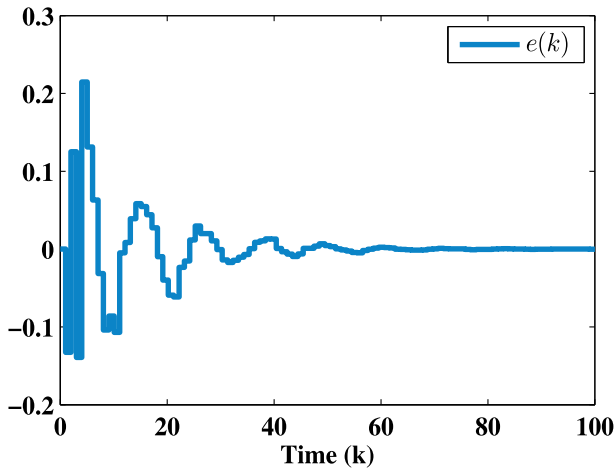


Fig. 14 Response of error system (36)

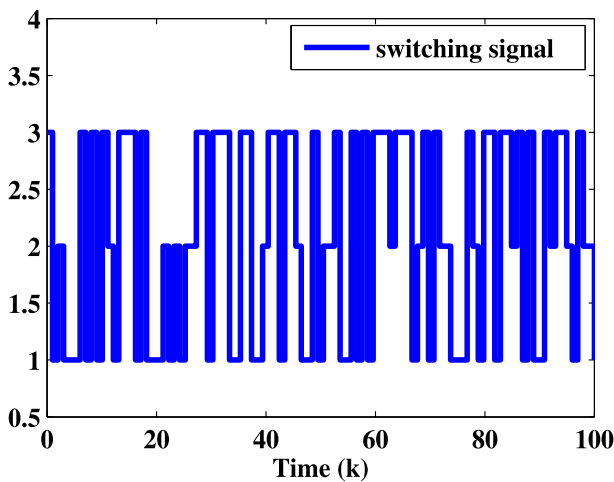


Fig. 15 Switching signal

ing estimates $\hat{x}_b(k)$ ($b = 1, 2, 3, 4$) are shown in Fig. 12. Further, the trajectories of the output $z(k)$ and its estimate $\hat{z}(k)$ are exhibited in Fig. 13. Besides, the response of error system with quantization of the augmented filtering error system (36) is shown in Fig. 14. The switching signals throughout the simulation process are depicted in Fig. 5. Finally, the time history of the filtering error system (36) is illustrated in Fig. 6. To be more specific, Fig. 6 clearly shows that the state trajectories lie within the obtained values σ_2 . Hence, it is evident that the addressed system (36) is stochastically finite-time bounded with $(\mathcal{X}, \mathcal{Y}, \mathcal{Z}) - \gamma$ dissipative performance index subject to $(0.2, 0.3946, 100, 0.3358, I, 0.1)$ under the proposed filtering problem.

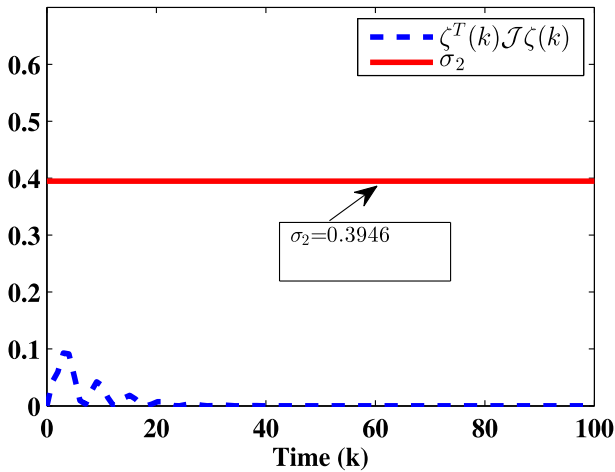


Fig. 16 Evolution of $\zeta^T(k) \mathcal{J} \zeta(k)$

5 Conclusion

In this work, the finite-time dissipative-based distributive non-fragile filter design problem is investigated for a class of discrete-time complex systems with multiple delays. Moreover, the sequences of stochastic variables are taken into account for the missing measurement phenomena which satisfies the Bernoulli distribution. In particular, the distributed filtering problem has been analyzed by designing the measured output over sensor nodes which includes dynamic quantization and missing phenomena for the addressed system. By applying \mathcal{S} -procedure lemma and Lyapunov–Krasovskii functional method, a finite-time distributed non-fragile filter has been designed such that the augmented filtering error system is stochastically finite-time bounded with prescribed $(\mathcal{X}, \mathcal{Y}, \mathcal{L}) - \gamma$ dissipative performance index over a finite period of time. Finally, three numerical examples including the CSTR model and a quarter-car suspension model are provided to prove the efficiency of the proposed distributive non-fragile filter design techniques.

Data Availability Data sharing is not applicable to this article as no new data were created or analyzed in this study.

References

1. X. Bu, H. Dong, F. Han, G. Li, Event-triggered distributed filtering over sensor networks with deception attacks and partial measurements. *Int. J. Gen. Syst.* **47**, 522–534 (2018)
2. D. Chen, C. Chen, J. Li, Fault detection filter design for a class of discrete-time impulsive switched systems with quantised signals. *Int. J. Syst. Sci.* **3**, 413–423 (2020)
3. Y. Chen, L. Yang, A. Xue, Finite-time passivity of stochastic Markov jump neural networks with random distributed delays and sensor nonlinearities. *Circuits Syst. Signal Process.* **38**, 2422–2444 (2019)

4. Z. Chen, J. Wu, Y. Xia, X. Zhang, Robustness of interdependent power grids and communication networks: a complex network perspective. *IEEE Trans. Circuits Syst. II Express Br.* **65**, 115–119 (2017)
5. D. Ding, Z. Wang, B. Shen, H. Dong, H_∞ state estimation with fading measurements, randomly varying nonlinearities and probabilistic distributed delays. *Int. J. Robust Nonlinear Control* **25**, 2180–2195 (2015)
6. H. Duan, T. Peng, Finite-time reliable filtering for $T - S$ fuzzy stochastic jumping neural networks under unreliable communication links. *Adv. Differ. Equ.* **1**, 1–7 (2017)
7. J. Foster, Prior commitment and uncertainty in complex economic systems: reinstating history in the core of economic analysis. *Scott. J. Polit. Econ.* **64**, 392–418 (2017)
8. A. Goel, A. Fekih, S. Mobayen, Fast non-singular terminal sliding controller for magnetic levitation systems: a disturbance-observer scheme, in *2020 American Control Conference (ACC)*, pp. 5059–5064 (2020)
9. X. He, W. Xue, X. Zhang, H. Fang, Distributed filtering for uncertain systems under switching sensor networks and quantized communications. *Automatica* **114**, 108842 (2020)
10. L. Hou, X. Zhao, H. Sun, G. Zong, $l_2 - l_\infty$ filtering of discrete-time switched systems via admissible edge-dependent switching signals. *Syst. Control Lett.* **113**, 17–26 (2018)
11. K.A. Kabir, K. Kuga, J. Tanimoto, The impact of information spreading on epidemic vaccination game dynamics in a heterogeneous complex network—a theoretical approach. *Chaos, Solitons Fractals* **132**, 109548 (2020)
12. J. Li, J.H. Park, D. Ye, Fault detection filter design for switched systems with quantisation effects and packet dropout. *IET Control Theory Appl.* **11**, 182–193 (2017)
13. W. Li, Y. Jia, J. Du, Distributed filtering for discrete-time linear systems with fading measurements and time-correlated noise. *Digit. Signal Process.* **60**, 211–219 (2017)
14. X. Lin, W. Zhang, Z. Yang, Y. Zou, Finite-time boundedness of switched systems with time-varying delays via sampled-data control. *Int. J. Robust Nonlinear Control* **30**, 2953–2976 (2020)
15. Y. Liu, Y. Qin, J. Huang, T. Huang, X. Yang, Finite-time synchronization of complex-valued neural networks with multiple time-varying delays and infinite distributed delays. *Neural Process. Lett.* **50**, 1773–1787 (2019)
16. S. Mobayen, C.K. Volos, S. Kaçar, Ü. Çavuşoslu, B. Vaseghi, A chaotic system with infinite number of equilibria located on an exponential curve and its chaos-based engineering application. *Int. J. Bifurc. Chaos* **9**, 1850112 (2018)
17. J. Mostafaei, S. Mobayen, B. Vaseghi, M. Vahedi, A. Fekih, Complex dynamical behaviors of a novel exponential hyper-chaotic system and its application in fast synchronization and color image encryption. *Sci. Prog.* **104**, 00368504211003388 (2021)
18. R. Sakthivel, R. Sakthivel, O.M. Kwon, P. Selvaraj, S.M. Anthoni, Observer-based robust synchronization of fractional-order multi-weighted complex dynamical networks. *Nonlinear Dyn.* **98**, 1231–1246 (2019)
19. S. Shamsirband, M. Fathi, A. Dehzangi, A.T. Chronopoulos, H. Alinejad-Rokny, A review on deep learning approaches in healthcare systems: taxonomies, challenges, and open issues. *J. Biomed. Inf.* **113**, 103627 (2020)
20. S. Shamsirband, S. Hashemi, H. Salimi, S. Samadianfard, E. Asadi, S. Shadkani, K. Kargar, A. Mosavi, N. Nabipour, K.W. Chau, Predicting standardized streamflow index for hydrological drought using machine learning models. *Eng. Appl. Comput. Fluid Mech.* **14**, 339–350 (2020)
21. L. Sheng, Y. Niu, M. Gao, Distributed resilient filtering for time-varying systems over sensor networks subject to Round-Robin/stochastic protocol. *ISA Trans.* **87**, 55–67 (2019)
22. B. Vaseghi, S.S. Hashemi, S. Mobayen, A. Fekih, Finite time chaos synchronization in time-delay channel and its application to satellite image encryption in OFDM communication systems. *IEEE Access* **9**, 21332–21344 (2021)
23. B. Vaseghi, S. Mobayen, S.S. Hashemi, A. Fekih, Fast reaching finite time synchronization approach for chaotic systems with application in medical image encryption. *IEEE Access* **9**, 25911–25925 (2021)
24. J. Wang, M. Chen, H. Shen, Event-triggered dissipative filtering for networked semi-Markov jump systems and its applications in a mass-spring system model. *Nonlinear Dyn.* **87**, 2741–2753 (2017)
25. J. Wang, F. Li, Y. Sun, H. Shen, On asynchronous $l_2 - l_\infty$ filtering for networked fuzzy systems with Markov jump parameters over a finite-time interval. *IET Control Theory Appl.* **10**, 2175–2185 (2016)
26. M. Wang, Y. Fang, Y. Luo, F. Yang, C. Zeng, W.L. Duan, Influence of non-Gaussian noise on the coherent feed-forward loop with time delay. *Chaos, Solitons Fractals* **129**, 46–55 (2019)

27. B. Wu, X.H. Chang, X. Zhao, Fuzzy H_∞ output feedback control for nonlinear NCSs with quantization and stochastic communication protocol. *IEEE Trans. Fuzzy Syst.* **29**, 2623–2634 (2021)
28. Z. Wu, B. Jiang, Y. Kao, Finite-time \mathcal{H}_∞ filtering for Itô stochastic Markovian jump systems with distributed time-varying delays based on optimisation algorithm. *IET Control Theory Appl.* **13**, 702–710 (2019)
29. W. Xia, Y. Li, Y. Chu, S. Xu, Z. Zhang, Dissipative filter design for uncertain Markovian jump systems with mixed delays and unknown transition rates. *Signal Process.* **141**, 176–186 (2017)
30. J. Xiong, X.-H. Chang, X. Yi, Design of robust nonfragile fault detection filter for uncertain dynamic systems with quantization. *Appl. Math. Comput.* **338**, 774–788 (2018)
31. X. Xue, H. Xu, L. Xu, Distributed filtering and control for time delay systems interconnected over an undirected graph. *Int. J. Control* **93**, 1839–1858 (2020)
32. H. Yan, F. Qian, F. Yang, H. Shi, H_∞ filtering for nonlinear networked systems with randomly occurring distributed delays missing measurements and sensor saturation. *Inf. Sci.* **370**, 772–782 (2016)
33. D. Zhang, W. Cai, Q.G. Wang, Energy-efficient H_∞ filtering for networked systems with stochastic signal transmissions. *Signal Process.* **101**, 134–141 (2014)
34. D. Zhang, P. Shi, W.A. Zhang, L. Yu, Energy-efficient distributed filtering in sensor networks: a unified switched system approach. *IEEE Trans. Cybern.* **47**, 1618–1629 (2017)
35. Y. Zhang, Y. Ou, Resilient dissipative filtering for uncertain Markov jump nonlinear systems with time-varying delays. *Circuits Syst. Signal Process.* **37**, 636–657 (2018)
36. M. Zhu, Y. Chen, Y. Kong, C. Chen, J. Bai, Distributed filtering for Markov jump systems with randomly occurring one-sided Lipschitz nonlinearities under Round-Robin scheduling. *Neurocomputing* **417**, 396–405 (2020)

Publisher's Note Springer Nature remains neutral with regard to jurisdictional claims in published maps and institutional affiliations.

Springer Nature or its licensor holds exclusive rights to this article under a publishing agreement with the author(s) or other rightsholder(s); author self-archiving of the accepted manuscript version of this article is solely governed by the terms of such publishing agreement and applicable law.